

Investigation of some processes of multiple lepton and boson birth on linear colliders of polarized photons.

T. Shishkina*

Abstract

The main possibilities of investigation of leptons and bosons birth in interaction of polarized photons are considered. The usage of $\gamma\gamma \rightarrow f\bar{f}[+\gamma]$ reactions for the luminosity measurement on linear photon collider is analyzed. The achievable precision of the luminosity measuring is considered and calculated. The first-order QED correction to $\gamma\gamma \rightarrow l\bar{l}$ scattering is analyzed. Differential cross section of process $\gamma\gamma \rightarrow 4l$ is calculated using the helicity amplitudes method as well as covariant method of precision calculations. All possible polarization states of interacting particles are investigated under different cuts of TESLA kinematics. For the detection of deviations from SM predictions at linear $\gamma\gamma$ colliders with centre of mass energies running to 1 TeV the influence of three possible anomalous couplings on the cross sections of W^+W^- productions has been investigated. The significant discrimination between various anomalous contributions is discovered. The main contribution of high order electroweak effects is considered.

1 Introduction

The Standard Model (SM) is able to describe all experimental data up to now with typical precision around one per mille. Nevertheless the Model is not the final theory valid up to very high scales and at linear collider that can run at centre of mass energies around 1 TeV one can hope to see finally deviations in precision measurements occur typically for two reasons.

If the new physics occurs in loop diagrams their effect is usually suppressed by a loop factor $\alpha/4\pi$ and very high precision is required to see it. If the new physics is already on the Born level but at very high masses the effects are suppressed by propagator factor $\frac{s}{s-m_{NP}^2-im_{NP}\Gamma}$ so that is important to work at the highest possible energies.

*BSU, Minsk

Both effects have already been used successfully in the past.

For example, ten years ago LEP could predict the mass of the top from its loop effects. It was found at TEVATRON with exactly such mass. In the same way it is hoped that in ten years from now a linear collider can obtain effects of new physics.

Linear lepton colliders will provide the opportunity to investigate photon collisions at energies and luminosities close to these in e^+e^- collisions [1].

The possibility to transform the future linear e^+e^- -colliders into the $\gamma\gamma$ and γe -colliders with approximately the same energies and luminosities was shown. The basic e^+e^- -colliders can be transformed into the $e\gamma$ - or $\gamma\gamma$ -colliders. The intense γ -beams for photon colliders are suggested to be obtained by Compton scattering of laser lights which is focused on electrons beams of basic e^+e^- -accelerators.

The electron and photon linear colliders of next generation will attack unexplored higher energy region where new behaviour can turn up. In this area the photon colliders have a number of advantages.

- The first of the above advantages is connected with the better signal/background ratio at both e^+e^- - and $e\gamma/\gamma\gamma$ -colliders in comparison with hadron ones.
- The production cross sections at photon colliders are usually larger than those at electron colliders.
- The photon colliders permit to investigate both of the problems of new physics and those ones of "classical" hadron physics and QCD.

So it is exclusively important task to use possibilities of $\gamma\gamma$ -colliders to realize the experiments of the next generation.

If a light Higgs exists one of the main tasks of a photon collider will be the measurement of the partial width $\Gamma(H \rightarrow \gamma\gamma)$. Not to be limited by the error from luminosity determination the luminosity of the collider at the energy of the Higgs mass has to be known with a precision of around 1%.

To produce scalar Higgses the total angular momentum of the two photons has to be $J=0$. In this case the cross section $\gamma\gamma \rightarrow l^+l^-$ is suppressed by factor m_l^2/s and thus not usable for luminosity determination.

In the SM the couplings of the gauge bosons and fermions are constrained by the requirements of gauge symmetry. In the electroweak sector this leads to trilinear and quartic interactions between the gauge bosons with completely specified couplings.

The trilinear and quartic gauge boson couplings probe different aspects of the weak interactions. The trilinear couplings directly test the non-Abelian gauge structure, and possible deviations from the SM forms have been extensively studied. In contrast, the quartic couplings can be regarded as a more direct way of consideration of electroweak symmetry breaking or, more generally, on new physics which couples to electroweak bosons.

In this respect it is quite possible that the quartic couplings deviate from their SM values while the triple gauge vertices do not. For example, if the mechanism for electroweak symmetry breaking doesn't reveal itself through the discovery of new particles such as the Higgs boson, supersymmetric particles or technipions it is possible that anomalous quartic couplings could provide the first evidence of new

physics in this sector of electroweak theory.

The production of several vector bosons is the best place to search directly for any anomalous behaviour of triple and quartic couplings.

We wait for colliders with higher center of mass energy in order to produce a final state with three or more gauge bosons and to test the quartic gauge-bosons couplings. The future project TESLA [2] is the real candidate for investigation of process three boson production.

Previously the cross sections for triple gauge bosons production in framework of the SM presented for e^+e^- -colliders and hadronic colliders.

By using of transforming a linear e^+e^- collider in a $\gamma\gamma$ collider, one can obtain very energetic photons from an electron or positron beams. Such machines as TESLA which will reach a center of mass energy $\sim 1000 GeV$ with high luminosity ($\sim 10^{33} cm^{-2}s^{-1}$) will be able to study multiple vector boson production with high statistics.

For obvious kinematic reasons, processes where at least one of the gauge bosons is a photon have the largest cross sections.

We examine the production of three vector boson in $\gamma\gamma$ collisions through the reaction

$$\gamma + \gamma \rightarrow W^+ + W^- + Z^0, \quad (1)$$

using beams of polarized photons.

1. This process involve only interactions between the gauge bosons making more evident any deviations from predictions of the SM gauge structure.

2. There is no tree-level contribution involving the Higgs boson which excludes all the uncertainties coming from the scalar sector.

We analyze the total cross section of the process of interaction of the two γ with fixed polarization, as well as the dynamical distributions of the final state vector bosons.

The measurement of cross section and asymmetries of this process is complementary to the analysis of the production of vector boson pairs.

So the photon linear colliders have the great physical potential [2, 3] (Higgs and SUSY particles searching, study of anomalous gauge boson couplings and hadronic structure of photons etc.). Performing of this set of investigations requires a fine measurement of the luminosity of photon beams. For this purpose some of the well-known and precisely calculated reactions (see, for example, $\gamma\gamma \rightarrow 2f, 4f$, [4, 5, 6, 7, 8, 9]) are traditionally used.

It was shown that it is convenient to use the events of $\gamma\gamma \rightarrow l^+l^-$ process for measuring the luminosity of the $J=2$ -beams (J is the total angular momentum of initial photon couple). Here l is the unpolarized light lepton (e or μ). It is the dominating QED process on $J=2$ beams and its events are easily detected.

The difficulties appear in the calibration of photon beams of similar helicity (the total helicity of $\gamma\gamma$ -system $J=0$) since the small magnitude of cross sections of the

most QED processes. For example, the leading term of cross section of $\gamma\gamma \rightarrow l\bar{l}$ scattering on $J=0$ -beams is of order α/π (≈ 0.002).

We have found that the exclusive reaction $\gamma\gamma \rightarrow l^+l^-\gamma$ provides the unique opportunity to measure the luminosity of $J=0$ beams on a linear photon collider.

One of the main purposes of the linear photon collider is the s -channel of the Higgs boson production at energies about $\sqrt{s} = 120\text{GeV}$ [2]. That is the reason of using this value of c.m.s. energy in our analysis.

2 Two lepton production with photon in $\gamma\gamma$ -collisions

The two various helicity configuration of the $\gamma\gamma$ -system leads to the different spectra of final particles and requires the two mechanisms of beam calibration. We have analyzed [4] the behaviour of the $\gamma\gamma \rightarrow l^+l^-\gamma$ reaction on beams with various helicities as a function of the parameters of detectors. We have performed the detail comparison of cross section on $\gamma^+\gamma^+$ ($J = 0$) and $\gamma^+\gamma^-$ -beams ($J = 2$). Since experimental beams are partially polarized the ratio of cross sections of $\gamma\gamma \rightarrow l^+l^-\gamma$ scattering on $J = 0$ to $J = 2$ -beams should be high for the effective luminosity measurement. We have outlined the conditions that greatly restrict the observation of the process on " $J = 2$ " beams, remaining the " $J = 0$ " cross section almost unchanged.

Finally we estimate the precision of luminosity measurement.

Consider the process

$$\gamma(p_1, \lambda_1) + \gamma(p_2, \lambda_2) \rightarrow f(p_1', e_1') + \bar{f}(p_2', e_2') + \gamma(p_3, \lambda_3), \quad (2)$$

where λ_i and e_i' are the photon and the fermion helicities.

We denote the c.m.s. energy squared by $s = (p_1 + p_2)^2 = 2p_1 \cdot p_2$, the final-state photon energy by w . For the differential cross section the normalized final-state photon energy (c.m.s. is used) $x = w/\sqrt{s}$ is introduced. The differential cross section $d\sigma/dx$ appears to be the energy spectrum of final-state photons.

The matrix elements are obtained using two methods: the massless helicity amplitudes [10] for the fast estimations and the exact covariant analysis [11] including finite fermion mass. Since final-state polarizations will not be measured we have summarized over all final particles helicities. The integration over the phase space of final particles is performed numerically using the Monte-Carlo method [12].

The calculations have been performed for various experimental restrictions on the parameters of final particles. Events are not detected if energies and angles are below the corresponding threshold values. The considering restrictions on the phase-space of final particles (the cuts) are denoted as follows:

- Minimum final-state photon energy: ω_{cut} ,
- Minimum fermions energy: $E_{f,cut}$,

- Minimum angle between any final and any initial particles (polar angle cut): Θ_{cut} ,
- Minimum angle between any pair of final particles: φ_{cut} .

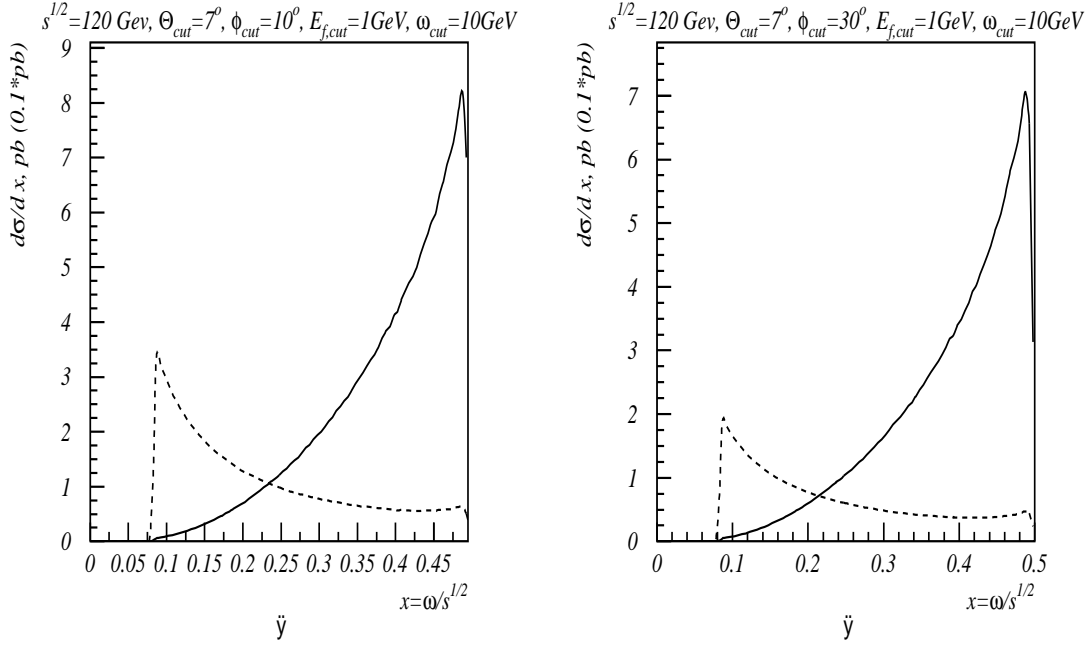


Figure 1: Final-state photon energy spectrum for $J = 0$ (solid) and $(J = 2) * 0.1$ (dotted) at $\sqrt{s} = 120\text{GeV}$ and cuts: $\Theta_{min} = 7^\circ$, $\varphi_{min} = 10^\circ$ (left) and $\varphi_{min} = 30^\circ$ (right), $E_{f,min} = 1\text{GeV}$, $\omega_{min} = 10\text{GeV}$.

Consider the energy spectrum of final photons. In fig. 1 the spectra for $J = 0$ and $(J = 2)$ are presented (the $(J = 2)$ -cross section is scaled on factor 0.1 for the convenience). The differential cross section $d\sigma/dx$ on $J = 2$ beams decreases while one on $J = 0$ beams raises with increasing of the final-state photon energy. This leads to the conclusion that if one increases the threshold on w , the process on $J = 2$ beams will be greatly restricted, but the rate of $J = 0$ events remains almost unchanged.

Next we analyze the total cross section dependence on the angular cuts Θ_{min} and φ_{min} (see figs. 2, 3). In $\gamma^+\gamma^-$ experiments ($J = 0$) the most of final fermions are radiated closely to the axis of initial photon (polar axis) and can't be detected. The $\gamma^+\gamma^-$ experiments ($J = 2$) have the large fraction of particles emitted at large angles. But they are likely emitted as the collinear fermion-photon pairs, that also can't be separated in the detector. The angular spectra of the final particles is represented in fig. 2. It shows that the rise of threshold on angle between final particles (up to 20°) restricts the $J = 2$ -cross section, while the $J = 0$ reaction is

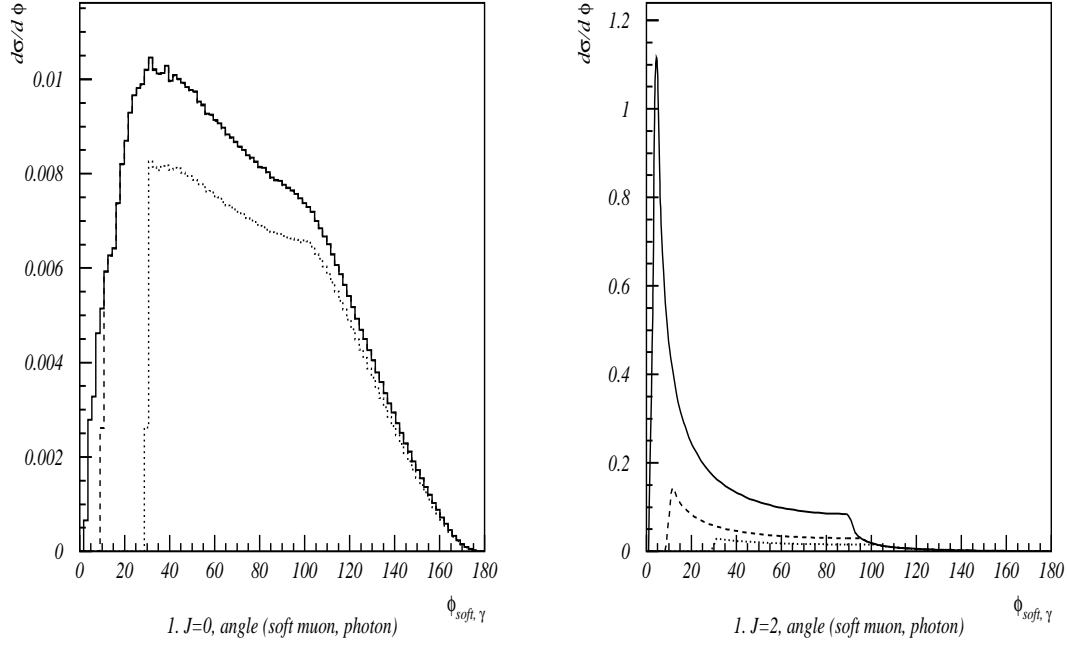


Figure 2: Angular plots (angle between fermion with lowest energy and final photon) at $\sqrt{s} = 120\text{GeV}$ at various sets of cuts: • $\Theta_{min} = 7^\circ$, $\varphi_{min} = 3^\circ$, $E_{f,min} = 1\text{GeV}$, $\omega_{min} = 1\text{GeV}$ (solid line); • $\Theta_{min} = 7^\circ$, $\varphi_{min} = 10^\circ$, $E_{f,min} = 1\text{GeV}$, $\omega_{min} = 10\text{GeV}$ (dashed line); • $\Theta_{min} = 7^\circ$, $\varphi_{min} = 30^\circ$, $E_{f,min} = 5\text{GeV}$, $\omega_{min} = 20\text{GeV}$ (dotted line).

almost unaffected.

It is clear that the ratio of these cross sections can be increased by reducing the polar angle cut Θ_{min} and by raising the collinear angle cut φ_{min} .

In fig. 3 we present the ratios of total cross sections $\sigma_{J=0}/\sigma_{J=2}$ depending on various of experimental cuts. Using also the graphs for spectra of final particles one can achieve the ratio $\sigma_{J=0}/\sigma_{J=2}$ up to 1 without sufficient decreasing of $\sigma_{J=2}$.

We have discovered the ratio of events on $J=0$ and $J=2$ beams strongly depends on the experimental cuts. We obtained the region (the configuration of cuts) where the processes on the both $J=0$ and $J=2$ beams have the cross sections close by each other. That is the region of small polar angle cut, high collinear angle cut as well as high minimal energy of final-state photons. At these parameters the total cross sections of $\gamma\gamma \rightarrow f\bar{f}\gamma$ in experiments using $\gamma^+\gamma^-$ and $\gamma^+\gamma^-$ beams appear to be the same order of magnitude.

The mass contribution is small in the great part of phase space of final particles. The most significant contribution is for the $J=0$ energy spectra (see fig. 4). The

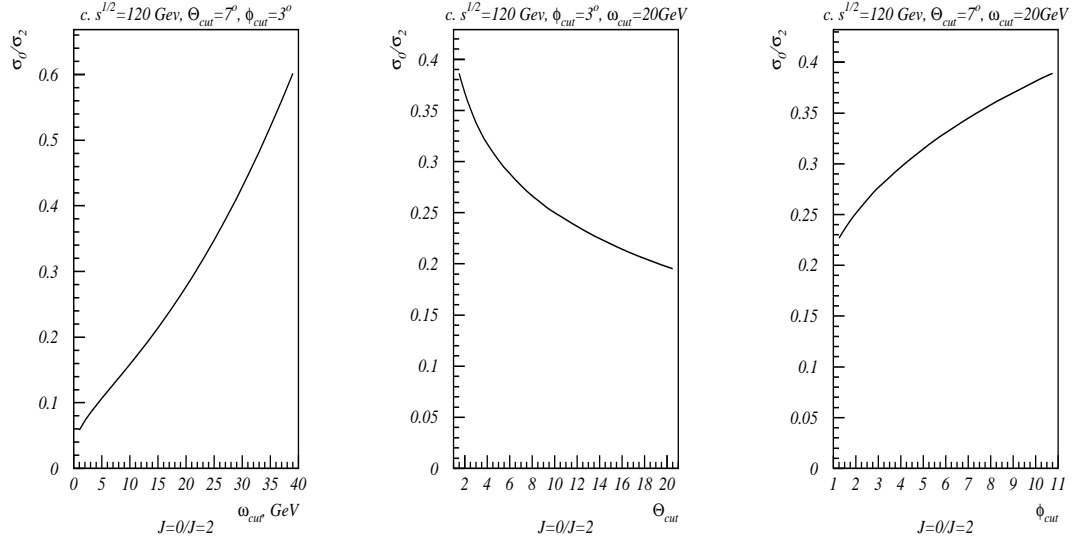


Figure 3: Ratios of total cross sections on $J = 0$ and $J = 2$ beams depending on different cuts.

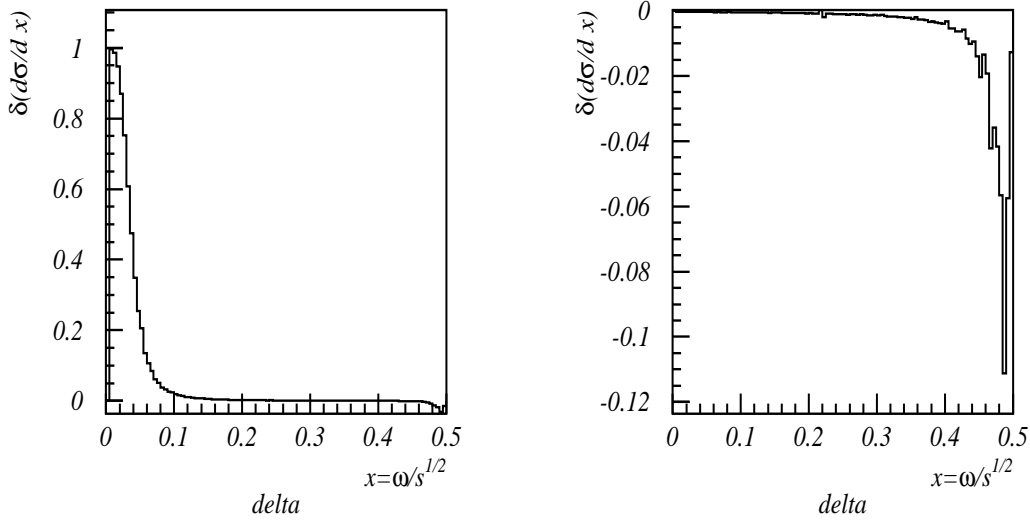


Figure 4: The relative mass contribution to energy spectra of final photon for $J=0$ (left) and $J=2$ (right) beams ($w_{cut}=1\text{GeV}$, $\mathcal{E}_{cut}=1\text{GeV}$, $\Theta_{cut}=7^\circ$, $\varphi_{cut}=3^\circ$).

high value of the contribution corresponds to regions where the differential cross section is minimal. The mass contribution to the total cross section is below the

1% level at any realistic set of cuts. It means that the helicity amplitudes is a good approach for study the $\gamma\gamma \rightarrow l^+l^-\gamma$ process.

2.1 Luminosity measurement of $J=0$ beams.

Finally, we analyze the precision of luminosity measurement [4] that can be achieved using the reaction $\gamma\gamma \rightarrow f\bar{f}\gamma$.

The most interest are offered by the two kinds of measurement. The first one is the measuring of beams luminosity with the wide energy spectrum. The second one is the same measurement for the narrow band around the energy of Higgs boson production.

We use for consideration the following TESLA project parameters [2]:

1. luminosity

$$\begin{aligned}\mathcal{L}(\sqrt{s'} > 0.8\sqrt{s'_{\max}}) &= 5.3 \cdot 10^{33} \text{cm}^{-2} \text{s}^{-1}, \\ \mathcal{L}(m_H \pm 1 \text{GeV}) &= 3.8 \cdot 10^{32} \text{cm}^{-2} \text{s}^{-1};\end{aligned}$$

2. polarization $\mathcal{P} \approx 90\%$.

Our calculations allow to choose the set of cuts with the high $J=0$ cross section and high ratio $\sigma_{J=0}/\sigma_{J=2}$: $\omega_{\text{cut}} = 20 \text{GeV}$, $E_{f,\text{cut}} = 5 \text{GeV}$, $\Theta_{\text{cut}} = 6^\circ$, $\varphi_{\text{cut}} = 30^\circ$. For these cuts the total cross sections have the following values:

$$\begin{aligned}\sigma(J=0) &= 0.82 \text{pb}, \\ \sigma(J=2) &= 1.89 \text{pb}.\end{aligned}$$

So for the precision of luminosity measurement in a 2 years run ($2 \cdot 10^7 \text{s}$) one can obtain:

$$\begin{aligned}\frac{\Delta\mathcal{L}}{\mathcal{L}}(\sqrt{s'} > 0.8\sqrt{s'_{\max}}) &= 0.35\%, \\ \frac{\Delta\mathcal{L}}{\mathcal{L}}(m_H \pm 1 \text{GeV}) &= 1.3\%.\end{aligned}$$

3 Lepton-antilepton production in high energy polarized photons interaction

The luminosity measurement at $J=2$ beams will be performed using the reaction $\gamma\gamma \rightarrow l^+l^-$. It has the great cross section that provides the number of events enough for the 0.1% precision of luminosity determination.

The main task is to calculate the cross section with maximal precision. For realization of this purpose we have calculated the complete one-loop QED radiative corrections to cross section of $\gamma\gamma \rightarrow l^+l^-$ process including the hard photon bremsstrahlung.

The major feature of $\gamma\gamma \rightarrow f\bar{f}$ process is the small value of cross section if the total angular momentum of $\gamma\gamma$ -beams equals zero.

We analyze both the angular spectra and the invariant distributions of final particles. The angular spectrum of final leptons is calculated in form $d\sigma/d\cos\Theta(p_l, p_\gamma)$. It is more convenient to use Lorentz-invariant results for the experimental reasons. Therefore we analyze the process $\gamma\gamma \rightarrow f\bar{f}[+\gamma]$ including $O(\alpha)$ -corrections using the method of covariant calculations [11]. The invariant differential cross section is calculated in the form $d\sigma/d(p_l - p_\gamma)^2$ and can be used in the arbitrary experimental configuration.

The detailed analysis of the $\gamma\gamma \rightarrow l^+l^-$ process can be found in the adjacent report in these proceedings [5].

For the measurement the luminosity of $J = 2$ beams one will use the events of $\gamma\gamma \rightarrow l^+l^-$ process. The precision of measurement the luminosity of $J = 2$ beams that can be achieved using $\gamma\gamma \rightarrow l^+l^-$ process can be calculated in the same way that one for $J = 0$ beams. We introduce the ω_{max} parameter for the maximal energy of bremsstrahlung photon that will still result the detection of single exclusive $\gamma\gamma \rightarrow l^+l^-$ event. For the supposed TESLA detector parameters ($\omega_{max} = 1GeV$, $E_{f,cut} = 1GeV$, $\Theta_{cut} = 7^\circ$) one can obtain:

$$\begin{aligned}\frac{\Delta\mathcal{L}}{\mathcal{L}}\left(\sqrt{s'} > 0.8\sqrt{s'_{\max}}\right) &= 0.04\%, \\ \frac{\Delta\mathcal{L}}{\mathcal{L}}(m_H \pm 1GeV) &= 0.1\%.\end{aligned}$$

The achieved precision is sufficient for the huge variety of experiments at the photon collider.

4 Production of four leptons in $\gamma\gamma$ electroweak interaction

Since the high accuracy and relatively clean environment are provided by a linear collider, a precision calculation of background including $\gamma\gamma \rightarrow (...) \rightarrow 4l$ process is necessary.

Total cross sections of such interactions have been already calculated and analyzed in refs. [13] about 30 years ago and were found to be large enough:

$$\begin{aligned}\sigma &= 6500nb \quad (\gamma\gamma \rightarrow 2e^-2e^+), \\ \sigma &= 5.7nb \quad (\gamma\gamma \rightarrow e^+e^-\mu^+\mu^-), \\ \sigma &= 0.16nb \quad (\gamma\gamma \rightarrow 2\mu^-2\mu^+).\end{aligned}$$

However these calculations have used the low energy approximation and obtained results are not applicable for modern high energy investigations.

There was applied the algorithm ALPHA [7] for automatic computations of scattering amplitude. However modern high energy experiments require the cross section calculation and analysis at fixed polarization states of initial and final particles that ALPHA method couldn't provide.

Our purpose was investigation of process $\gamma\gamma \rightarrow 4l$ using parameters of linear colliders of new generation such as TESLA [2].

There are six topographically different Feynman diagrams of electroweak interactions for describing of this process (see fig. 5). Using C-, P- and crossing symmetries one can built 40 different diagrams.

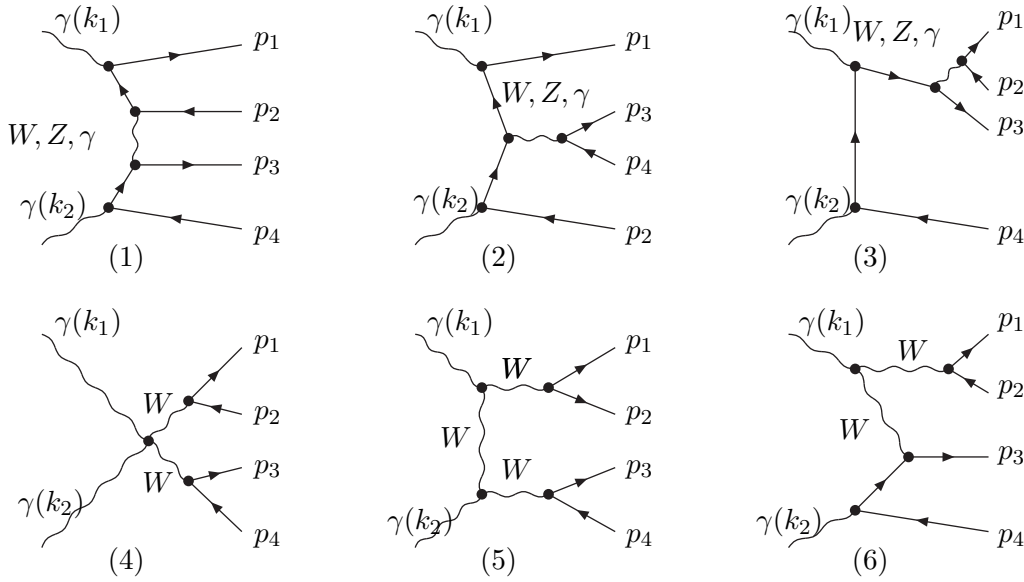


Figure 5: The Feynman diagrams of four lepton production in $\gamma\gamma$ electroweak interaction.

The diagrams containing charged current exchange are excluded because only processes with four charged leptons in the final state are considered.

The corresponding cross section has the form:

$$\sigma = \frac{1}{4(k_1 k_2)} \int |M|^2 d\Gamma. \quad (3)$$

Here $M = \sum_{i=1}^3 M_i$, M_i are the matrix elements of remaining diagrams (1)-(3) in fig. 5 and $d\Gamma$ is the phase space element.

Squared matrix element is constructed using the method of helicity amplitudes [10] as well as the method of precision covariant calculation [11]. The first one allows to calculate matrix element directly for each definite polarization state of initial and final particles. Amplitude constructed by this method contains only invariants without any bispinor, so many difficulties at squaring and numerical integration are excluded.

The explicit form of all matrix elements constructed using helicity amplitude method one can found in ref. [9].

The method of precision covariant calculations allows to obtain matrix element without any approximations and was used for verifying results in each step of our construction and calculation.

For the investigation of total and differential cross section the method of Monte-Carlo integration was applied. If two or more produced particles propagate into very close direction, the square of matrix element becomes very large (so-called collinear peaks problem). For the achievement of high precision the Monte-Carlo generator was adopted. Despite regular distributions of kinematic variables (such distributions usually applied into Monte-Carlo generators) we have used irregular one, which is very close to matrix element behavior. This proximity can be achieved by choosing of several free parameters available in the distribution function. So the adopted method of Monte-Carlo integration leads to results with very small numerical error, nearly $(0.1\% - 0.2\%)$. The accuracy of the method of helicity amplitude was investigated. It was arrived at a decision that the results of two discussed methods have good agreement.

Some results, obtained for spin averaged differential cross section of electromagnetic $\gamma\gamma$ - interaction, can be seen in figs. 6 and 7. As it was expected, the total and differential cross sections have very strong dependence upon kinematic cuts on polar angle (the angle between directions of initial and final particles). We have found the magnitude of differential cross section increases significantly at polar angle tends to 0 or π . The cross section raises with decreasing of interaction particles energy. It has symmetric (asymmetric) form in case of similar (different) spin configuration of scattering photons. The cross section dependence on angle between initial photon momentum and a set of final particles directions has the same form due to electromagnetic interaction results are only presented.

5 The SM and anomalous amplitudes of $\gamma\gamma \rightarrow W^+W^-$

Future high-energy linear e^+e^- -colliders in $\gamma\gamma$ -mode could be a very useful instrument to explore the mechanism of symmetry breaking in electroweak interaction. $\gamma\gamma$ -colliders give the opportunity for measurement of a light Higgs productions on resonance and $H\gamma\gamma$ coupling because of the processes $\gamma\gamma \rightarrow H \rightarrow ZZ, b\bar{b}, WW$. In the case of heavy mass Higgs bosons (over 1 TeV) a huge background from $\gamma\gamma \rightarrow W_T^+W_T^-$ complicates a search of the Higgs signal.

Another way to probe the symmetry breaking is examination of the self couplings of the W, Z bosons in non-minimal gauge models. Since the cross section of $\gamma\gamma \rightarrow W^+W^-$ is large the WW -production would be provided mainly by $\gamma\gamma$ scattering [14]. So the Born cross section $\sigma(\gamma\gamma \rightarrow WW)$ is about 110 pb at 1 TeV on unpolarized γ -beams at that all contributions of different polarization sets of W -bosons are

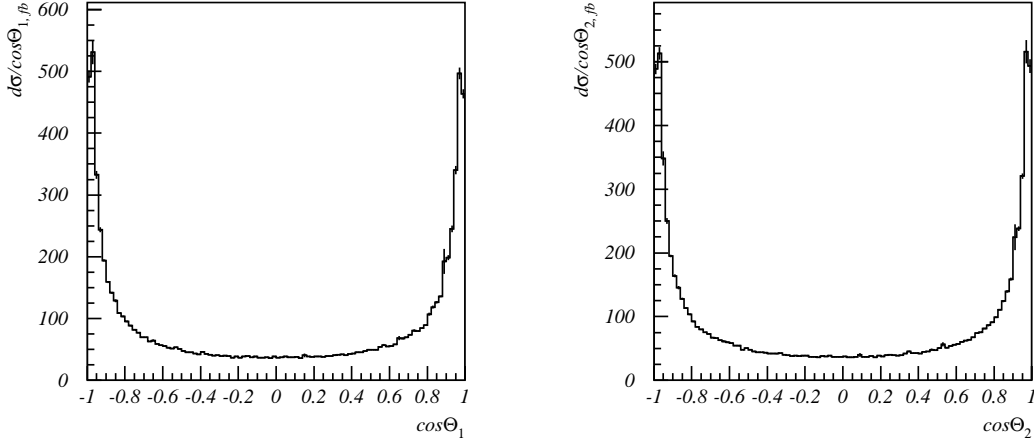


Figure 6: Spin averaged differential cross section of $\gamma\gamma \rightarrow 4l$ process at energy of interaction beams 1 TeV in c.m.s. θ_1 (θ_2) is the angle between directions of the first (second) photon and the first lepton. The magnitude of polar angle cut is equal to 7° .

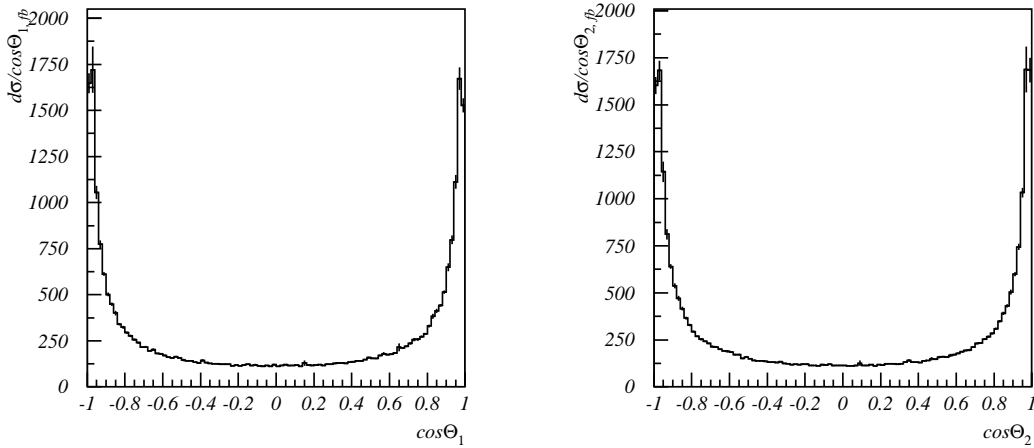


Figure 7: Spin averaged differential cross section of $\gamma\gamma \rightarrow 4l$ process at energy of interaction beams 500 GeV in c.m.s. θ_1 (θ_2) is the angle between directions of the first (second) photon and the first lepton. The magnitude of polar angle cut is equal to 7° .

considered. Corresponding cross section of WW -production in e^+e^- collisions is an order of magnitude smaller and amount to 10 pb at the same circumstances.

In addition to the $\gamma\gamma \rightarrow W^+W^-$ process one needs to consider a reaction of $\gamma\gamma \rightarrow W^+W^-Z$ because of its cross section becomes about 5% – 10% of the $\sigma(\gamma\gamma \rightarrow WW)$ at energies $\sqrt{s} \geq 500 \text{ GeV}$. The anomalous tri-linear γWW , ZWW [15] and quartic $\gamma\gamma WW$, γZWW , $ZZWW$ [16] couplings induce deviations of Born cross sections $\sigma(\gamma\gamma \rightarrow WW)$ and $\sigma(\gamma\gamma \rightarrow WWZ)$ from Standard Model values.

In order to evaluate contributions of anomalous couplings a cross section of $\gamma\gamma \rightarrow W^+W^-$ must be calculated with a high precision. Therefore one needs to calculate the main contribution of high order electroweak effects: one-loop correction, real photon and Z -boson emission.

The amplitude of $\gamma\gamma \rightarrow W^+W^-$ are defined as follows

$$M = G_v \epsilon_\mu(k_1) \epsilon_\nu(k_2) \epsilon_\alpha(p_+) \epsilon_\beta(p_-) M_T^{\mu\nu\alpha\beta}, \quad (4)$$

where k_1, k_2, p_+, p_- are 4-momenta of the γ, γ, W^+, W^- respectively, and $\epsilon_\mu(k_1), \epsilon_\nu(k_2), \epsilon_\alpha(p_+), \epsilon_\beta(p_-)$ – 4-vectors of polarizations accordingly. The constant G_v is equal to $e^3 \cot \theta_W$. The total amplitude M_T is defined by amplitudes M_i ($i = 1, 3$) corresponding to the Feynman diagrams, presented in fig. 8:

$$M_T^{\mu\nu\alpha\beta} = \sum_{i=1}^3 M_i^{\mu\nu\alpha\beta}. \quad (5)$$

These three amplitudes are constructed from a trilinear boson $\Gamma_3^{\mu\alpha\beta}$, a quartic boson

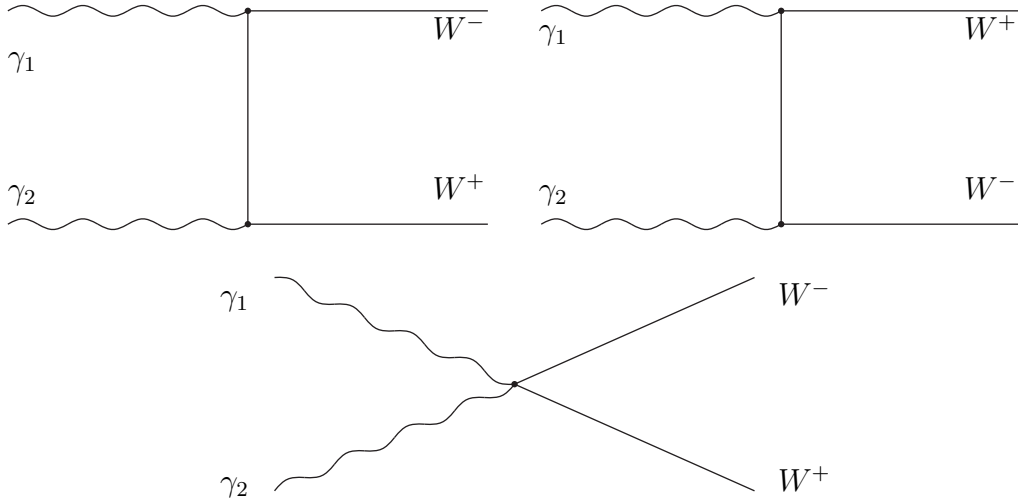


Figure 8: The Feynman diagrams for W^+W^- -production

$\Gamma_4^{\mu\nu\alpha\beta}$ vertices and a boson propagator $D_{\alpha\beta}(p)$, where p is 4-momentum of a virtual W -boson.

$$M_1^{\mu\nu\alpha\beta} = \Gamma_3^{\mu\alpha\xi}(-k_1, p_+) D_{\xi\lambda}(p_+ - k_1) \Gamma_3^{\nu\beta\lambda}(-k_2, p_-), \quad (6)$$

$$M_2^{\mu\nu\alpha\beta} = \Gamma_3^{\mu\beta\xi}(-k_1, p_-) D_{\xi\lambda}(p_- - k_1) \Gamma_3^{\nu\alpha\lambda}(-k_2, p_+), \quad (7)$$

$$M_3^{\mu\nu\alpha\beta} = \Gamma_4^{\mu\nu\alpha\beta}. \quad (8)$$

Consider the anomalous quartic boson vertices only. For this purpose the following 6-dimensional $SU(2)_c$ Lagrangians [17, 18] have been chosen

$$\begin{aligned} \mathcal{L}_0 &= -\frac{e^2}{16\Lambda^2} a_0 F^{\mu\nu} F_{\mu\nu} \bar{W}^\alpha \bar{W}_\alpha, \\ \mathcal{L}_c &= -\frac{e^2}{16\Lambda^2} a_c F^{\mu\alpha} F_{\mu\beta} \bar{W}^\beta \bar{W}^\alpha, \\ \tilde{\mathcal{L}}_0 &= -\frac{e^2}{16\Lambda^2} \tilde{a}_0 F^{\mu\alpha} \tilde{F}_{\mu\beta} \bar{W}^\beta \bar{W}^\alpha, \end{aligned} \quad (9)$$

where the triplet of gauge bosons \bar{W}_μ

$$\bar{W}_\mu = \left(\frac{1}{\sqrt{2}}(W_\mu^+ + W_\mu^-), \frac{i}{\sqrt{2}}(W_\mu^+ - W_\mu^-), \frac{1}{\cos\theta_W} Z_\mu \right) \quad (10)$$

and the field-strength tensors

$$F_{\mu\nu} = \partial_\mu A_\nu - \partial_\nu A_\mu, \quad W_{\mu\nu}^i = \partial_\mu W_\nu^i - \partial_\nu W_\mu^i, \quad \tilde{F}_{\mu\nu} = \frac{1}{2} \epsilon_{\mu\nu\rho\sigma} F^{\rho\sigma} \quad (11)$$

are introduced. The scale Λ keeps the coupling constant a_i dimensionless. In our calculations Λ are fixed by value of M_W (~ 80 GeV). As one can see the operators \mathcal{L}_0 and \mathcal{L}_c are C -, P -, CP -invariant. $\tilde{\mathcal{L}}_0$ is the P - and CP -violating operator. Then anomalous quartic boson vertices could be defined as

$$\begin{aligned} \Gamma_{4a_0}^{\mu\nu\alpha\beta}(k_1, k_2) &= \frac{1}{8\Lambda^2} (4a_0 g^{\alpha\beta} ((k_1 k_2) g^{\mu\nu} - k_1^\nu k_2^\mu)), \\ \Gamma_{4a_c}^{\mu\nu\alpha\beta}(k_1, k_2) &= \frac{1}{8\Lambda^2} \left(a_c ((k_1^\alpha k_2^\beta + k_1^\beta k_2^\alpha) g^{\mu\nu} + (k_1 k_2) (g^{\mu\alpha} g^{\nu\beta} + g^{\nu\alpha} g^{\mu\beta}) - \right. \\ &\quad \left. - k_1^\nu (k_2^\beta g^{\mu\alpha} + k_2^\alpha g^{\mu\beta}) - k_2^\nu (k_1^\beta g^{\mu\alpha} + k_1^\alpha g^{\mu\beta})) \right), \\ \Gamma_{4\tilde{a}_0}^{\mu\nu\alpha\beta}(k_1, k_2) &= \frac{1}{8\Lambda^2} (4\tilde{a}_0 g^{\alpha\beta} k_{1\rho} k_{2\sigma} \epsilon^{\mu\rho\nu\sigma}). \end{aligned} \quad (12)$$

The anomalous quartic boson vertices depend on the 4-momenta k_1, k_2 of the photons involved in the vertex.

Total cross section of $\gamma\gamma \rightarrow W^+W^-$ is calculated as

$$\sigma_{\lambda_1\lambda_2\lambda_3\lambda_4} = \frac{1}{2S} \int |M_{\lambda_1\lambda_2\lambda_3\lambda_4}|^2 d\Gamma^{(2)}, \quad (13)$$

where $M_{\lambda_1\lambda_2\lambda_3\lambda_4}$ have been defined in eq. (4), $d\Gamma$ is two-particle phase space of the bosons.

Through the method of Monte-Carlo integration [12] one may obtain numerical values of the cross section [19]. For these purposes the events generator has been built.

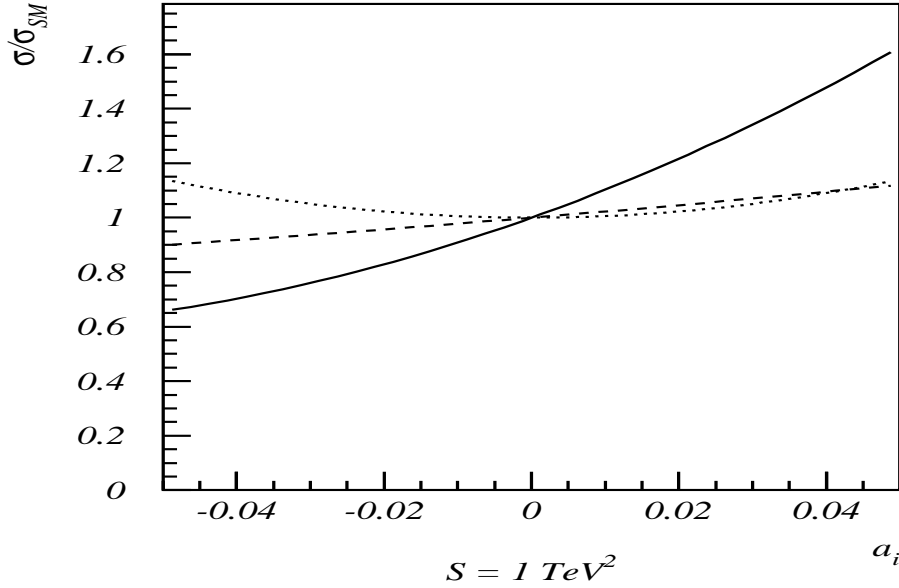


Figure 9: The comparison of the dependency of the cross sections $\sigma(W^+W^-)$. Solid line presents a_0 -, dashed line – a_c -, dotted line – \tilde{a}_0 -dependence

Fig. 9 shows the dependence of three total cross sections $\sigma(W^+W^-)$ on anomalous parameters. Graphs presented on the picture allow to value contributions of anomalous parts to the cross section. The fact that the minima of the curves are close to the SM point $a_i = 0$ means that the interference between the anomalous and the standard part of the matrix element is very small. Though the region of a_i is small, it's about 0.05, the cross section with anomalous constants may reach the values of 1.6σ . That stands for the evidence of great sensitivity of the cross section $\sigma(W^+W^-)$ to anomalous couplings. Taking into account a luminosity \mathcal{L} of photons about $100fb^{-1}/year$, energy $\sqrt{s} \sim 1TeV$ that corresponds to TESLA [2], statistical error will be equal to 0.05%. Therefore we can estimate bounds imposed on anomalous couplings to compare anomalous effect with statistical error. Contour plots on two non-zero anomalous constant, figs. 10–13, clearly demonstrate these bounds.

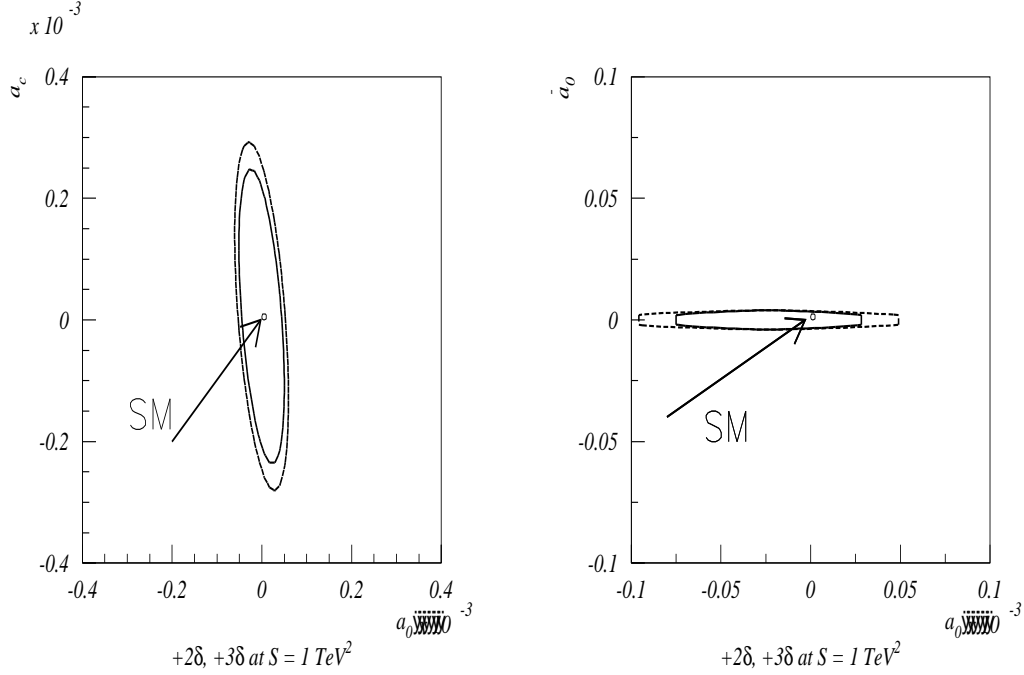


Figure 10: Contour plots on (a_0, a_c) for Figure 11: Contour plots on (a_0, \tilde{a}_0) for $+2\delta, +3\delta$ deviations of $\sigma(W^+W^-)$ $+2\delta, +3\delta$ deviations of $\sigma(W^+W^-)$

5.1 $\mathcal{O}(\alpha)$ correction to anomalous constants

Obviously a precision analysis of $\gamma\gamma \rightarrow WW$ at the future high energy $\gamma\gamma$ -colliders is impossible without calculation of whole set the first-order $\mathcal{O}(\alpha)$ radiative corrections, including real photon emission as well as a set of one-loop diagrams of $\gamma\gamma \rightarrow W^+W^-$ that are presented in fig.1 and fig.2 of ref. [20]. Inclusive cross section of the W pair production in the $\gamma\gamma$ collisions to the third order in α is given by the sum of Born cross section, interference term between the Born and one-loop amplitudes and cross section of the $WW\gamma$ production. In case of energy of $\gamma\gamma$ -interaction exceeds threshold of three boson production these process ($\gamma\gamma \rightarrow W^+W^-Z$) must be considered as radiative correction:

$$d\sigma(\gamma\gamma \rightarrow W^+W^-) = d\sigma^{Born}(\gamma\gamma \rightarrow W^+W^-) + \frac{1}{S} Re(M^{Born} M^{1-loop*}) d\Gamma^{(2)} + d\sigma^{soft}(\gamma\gamma \rightarrow W^+W^-\gamma) + d\sigma^{hard}(\gamma\gamma \rightarrow W^+W^-\gamma) + d\sigma^Z(\gamma\gamma \rightarrow W^+W^-Z). \quad (14)$$

Since one-loop and soft photon emission amplitudes are IR-divergent and only their sum is IR-finite it is convenient to consider soft and hard photon emissions separately. $d\sigma^{soft}$ can be presented by factorizable expression

$$d\sigma^{soft}(\gamma\gamma \rightarrow W^+W^-\gamma) = d\sigma^{Born}(\gamma\gamma \rightarrow W^+W^-) R^{soft}(\omega), \quad (15)$$

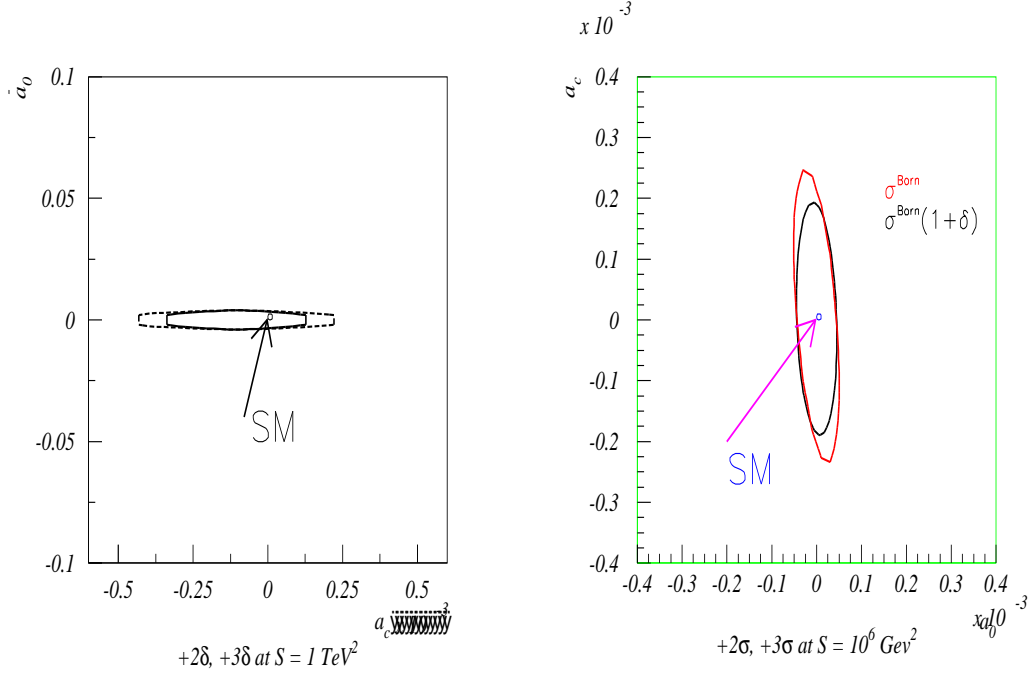


Figure 12: Contour plots on (a_c, \tilde{a}_0) for $+2\delta, +3\delta$ deviations of $\sigma(W^+W^-)$ Figure 13: Contour plots on (a_c, \tilde{a}_0) for $+2\delta$ deviations of $\sigma(W^+W^-)$

where ω is soft photon energy cutoff, $\beta = \sqrt{1 - 4m_W^2/s}$. The differential cross section of hard photon emission is given by

$$d\sigma^{\text{hard}}(\gamma\gamma \rightarrow W^+W^-\gamma) = d\sigma(\gamma\gamma \rightarrow W^+W^-\gamma) - d\sigma^{\text{soft}}(\gamma\gamma \rightarrow W^+W^-\gamma) \quad (16)$$

and can not be factorized. $d\sigma^{\text{soft}}$ and $d\sigma^{\text{hard}}$ present two contributions independent from infrared divergence as well as from soft photon cutoff.

One-loop amplitude M^{1-loop} were built due to usage of SCA (Algebra of Symbolic Calculations) programs (*MATHEMATICA*, *REDUCE*...) and transformations of scalar and tensor integrals to one-, two-, ..., six-point integrals. Cross section of WWZ production on $\gamma\gamma$ beams are obtained through application of the Monte-Carlo method of numerical integration and exact covariant expressions of $\gamma\gamma \rightarrow W^+W^-Z$ amplitudes. Cross section of $\gamma\gamma \rightarrow W^+W^-$ including the lowest-order QED radiative correction and three-boson production one can see in refs. [19, 20, 21].

Contour plot on a_0 and a_c of $\sigma(WW)$ with the lowest order QED correction are presented in figs. 10-13.

6 Conclusion

We have analyzed the possible usage of $\gamma\gamma \rightarrow f\bar{f}\gamma$ reaction for the luminosity measurement at $J=0$ beams on linear photon collider. The achievable precision of the luminosity measuring is considered and calculated. The optimal conditions for that measurement are found (for the high magnitude of $J=0$ cross section and small $J=2$ background). The first-order QED correction to $\gamma\gamma \rightarrow l\bar{l}$ cross section is calculated and analyzed at $J=2$ -beams.

The considered process gives the excellent opportunity for luminosity measurements with substantial accuracy.

The cross section of process of four charged lepton production are obtained in frame of method of helicity amplitudes as well as method of covariant calculations. Comparative analysis are performed. Monte-Carlo generator was developed to calculate differential and total cross section of four lepton production.

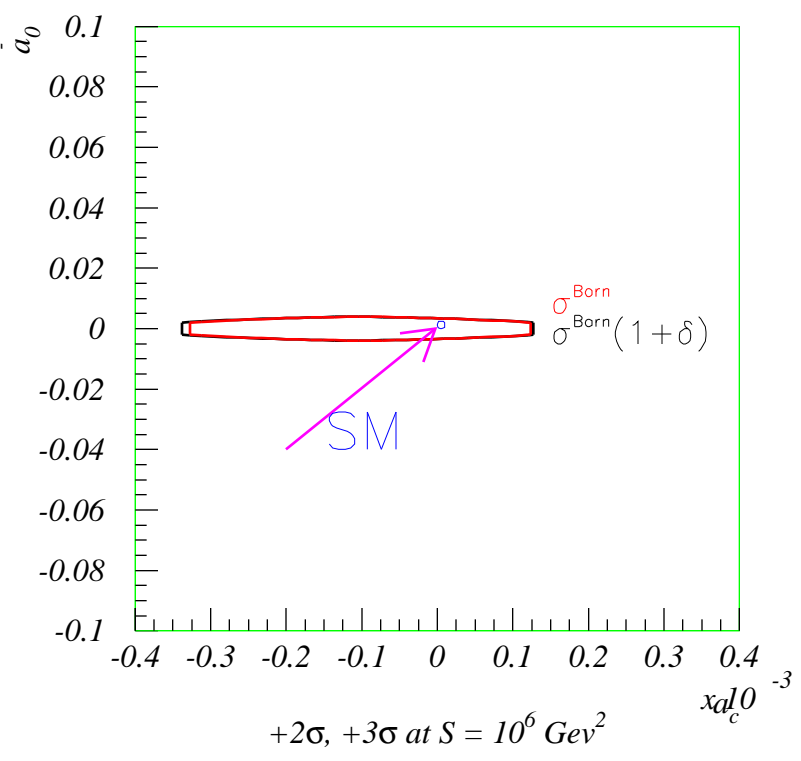
The investigation of the sensitivity of process of $\gamma\gamma \rightarrow W^+W^-$ and $\gamma\gamma \rightarrow W^+W^-Z$ to genuine anomalous quartic couplings a_0 , a_c and \tilde{a}_0 was performed at center-of-mass energy $\sqrt{s} = 1\text{ TeV}$. It was discovered that two-boson production has great sensitivity to anomalous constants a_c and a_0 but process $\gamma\gamma \rightarrow W^+W^-Z$ is more suitable for study of \tilde{a}_0 .

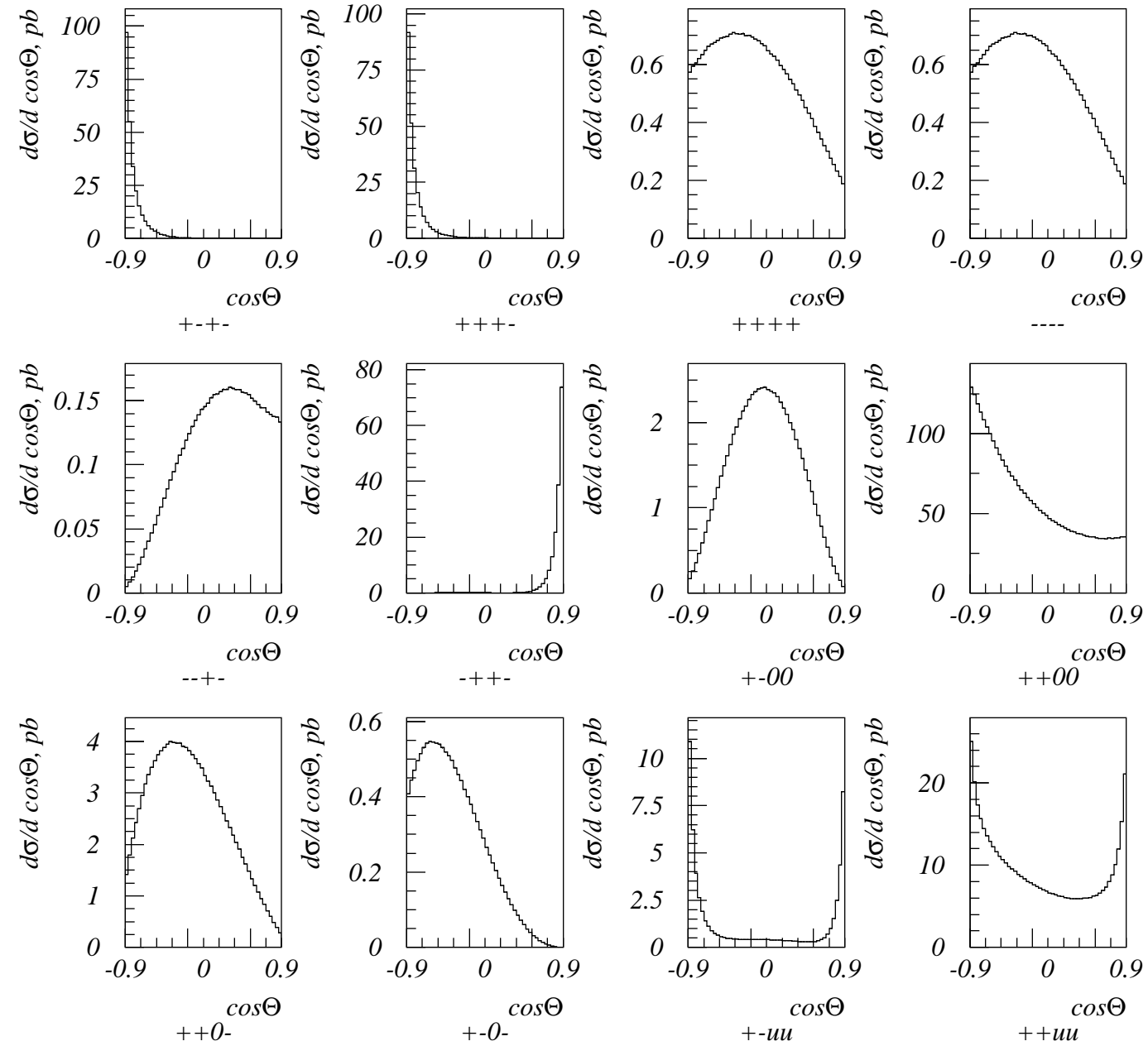
The fact that the minimum of the curves are close to the SM point $a_i = 0$ demonstrates the small value of the anomalous and the standard part interference. The first-order radiative correction to cross section $\sigma(\gamma\gamma \rightarrow W^+W^-)$ has significant magnitude and its calculation increases the precision of the a_0 and a_c measurement.

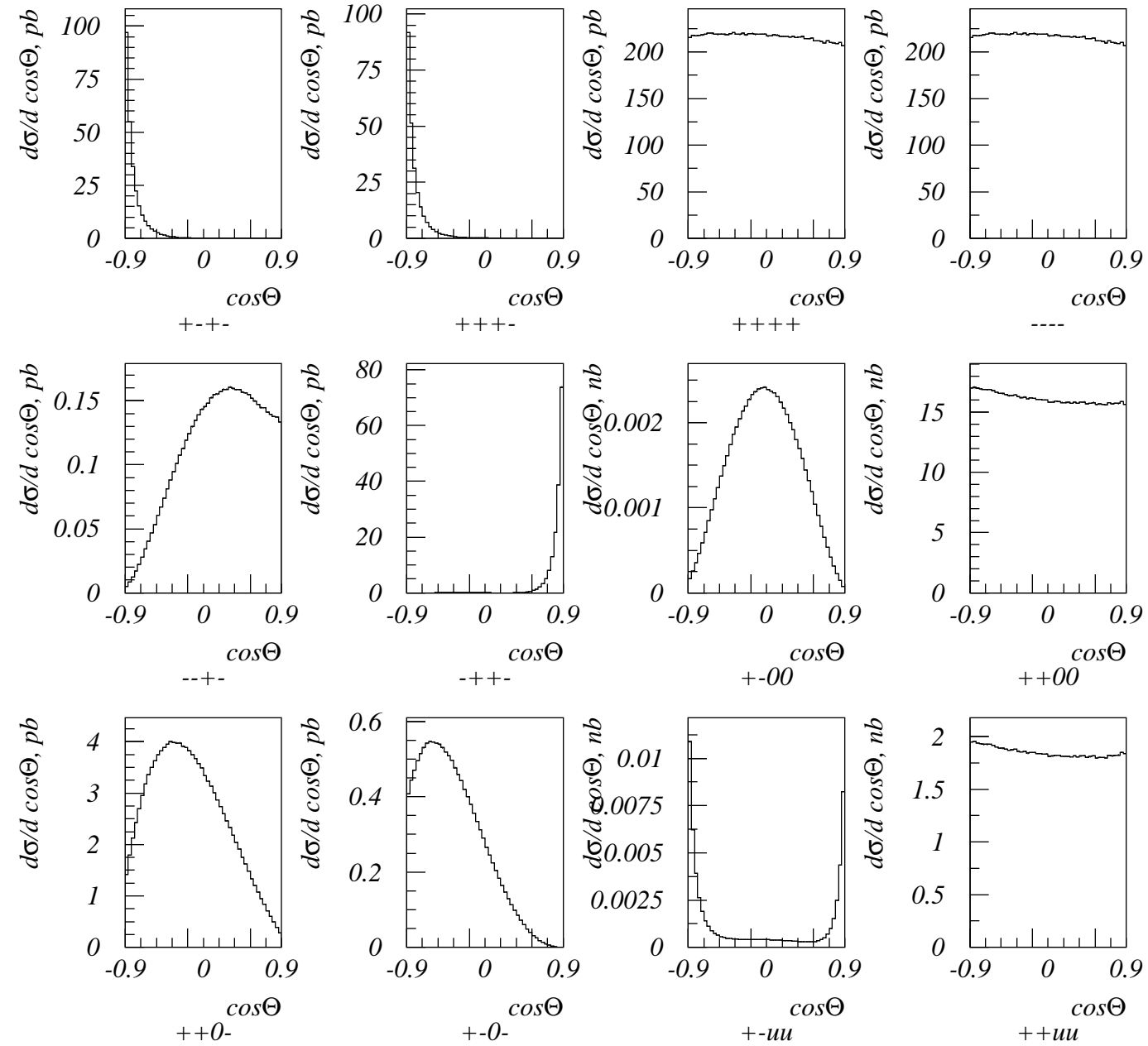
References

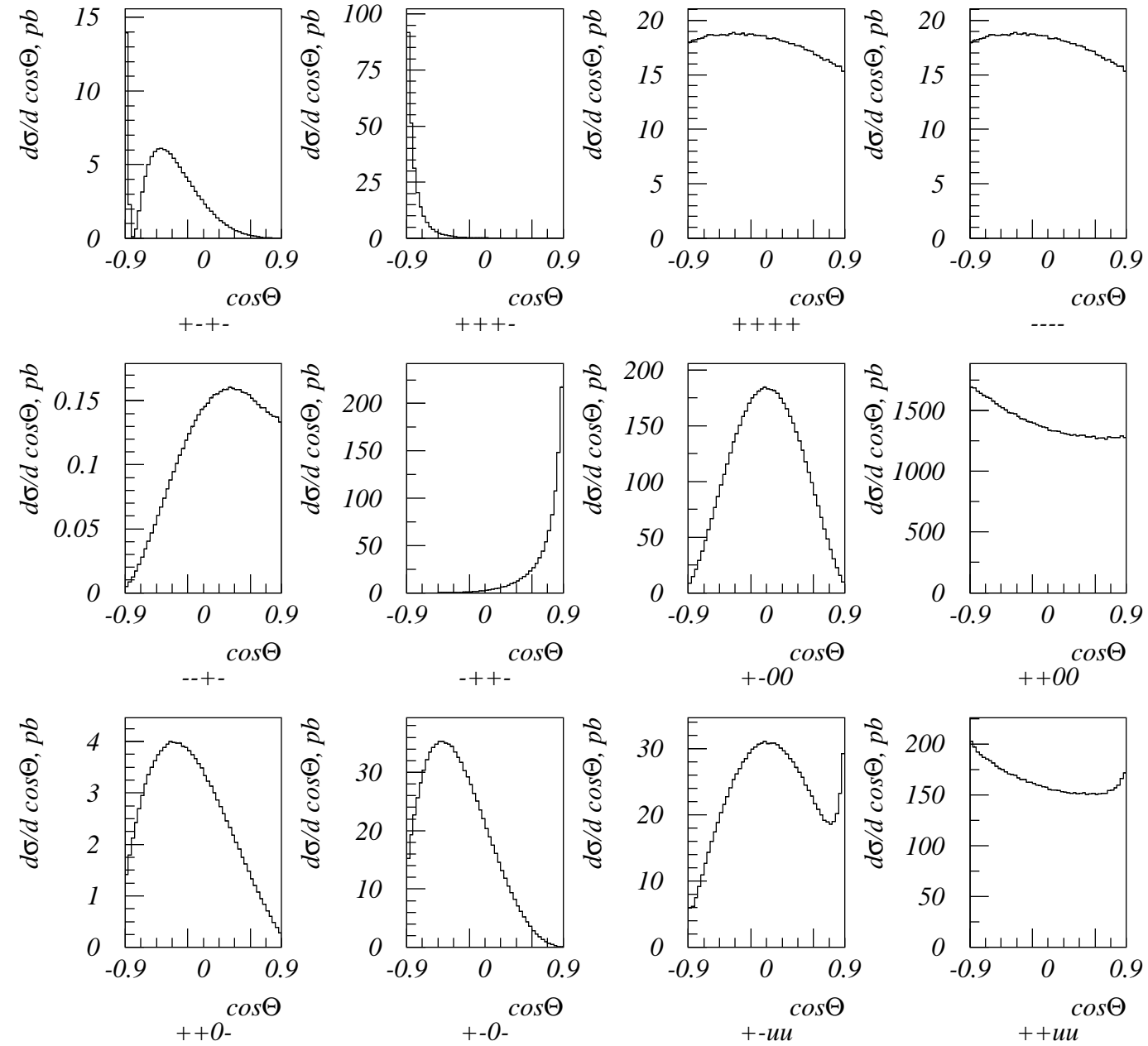
- [1] I. F. Ginzburg, G. L. Kotkin, V. G. Serbo and V. I. Telnov, Nucl. Instr. Meth. 205 (1983) 47;
I. F. Ginzburg, G. L. Kotkin, S. L. Panfil, V. G. Serbo and V. I. Telnov, Nucl. Instr. Meth. 219 (1984) 5.
- [2] B. Badelek *et al.*, *TESLA Technical Design Report Part VI: The Photon Collider at TESLA*, DESY-01-011E, hep-ex/0108012.
- [3] E. A. Kuraev, M. V. Galynskii, M. I. Levchuk, Phys. Part. Nucl. **31** (2000) 76, Fiz. Elem. Chast. Atom. Yadra 31 (2000) 155;
V. Telnov, Nucl. Instr. Meth. A494 (2002) 35, hep-ex/0207093.
- [4] T. V. Shishkina, V. V. Makarenko, hep-ph/0212409;
V. Makarenko, K. Mönig, T. Shishkina, Eur. Phys. J. C30, d01 (2003) 011, LC-PHSM-2003-016, hep-ph/0306135;
V. V. Makarenko, T. V. Shishkina, hep-ph/0310104.

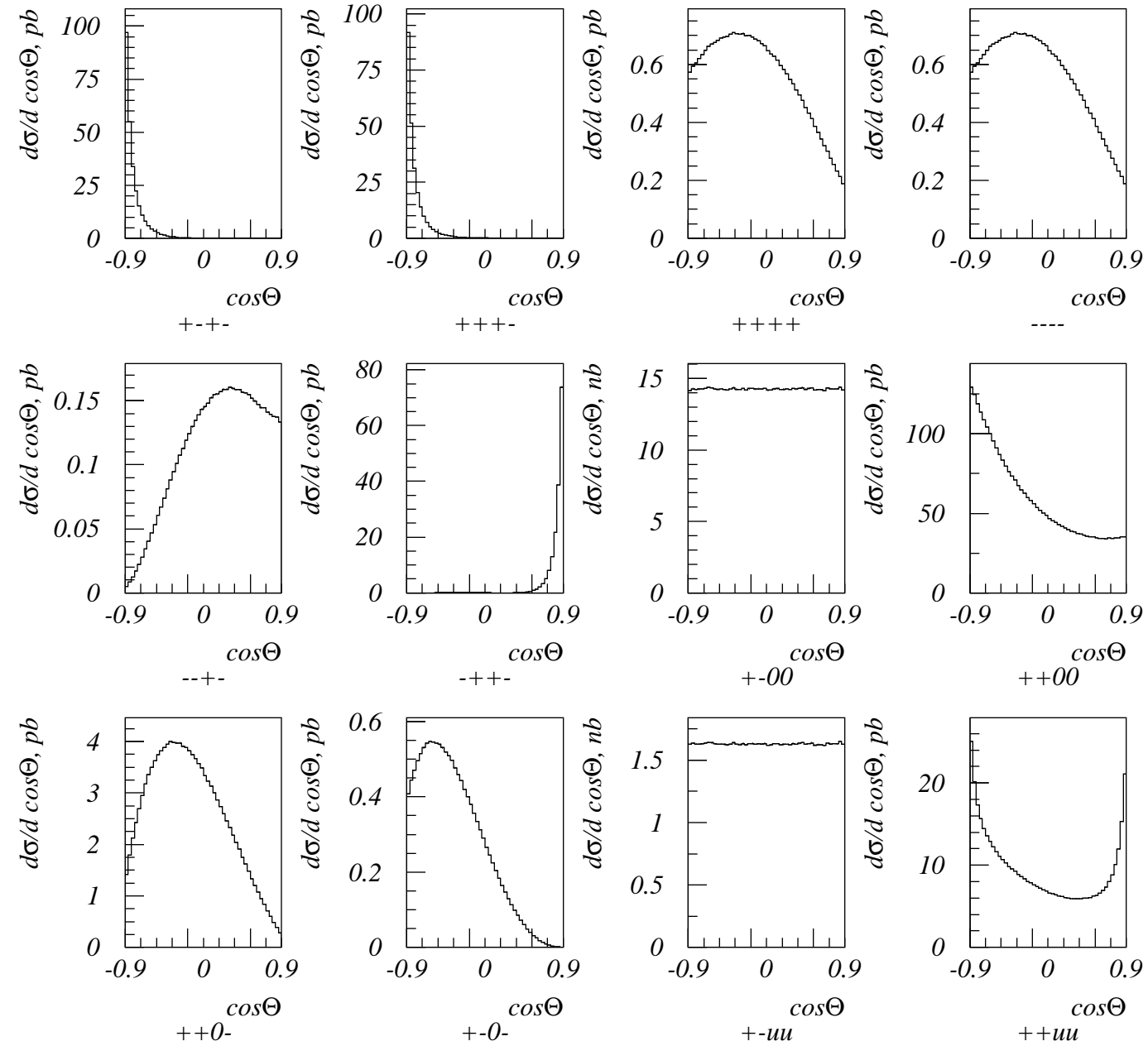
- [5] V. V. Makarenko, T. V. Shishkina, *The covariant first-order QED corrections to the fermion pair production in $\gamma\gamma$ -collisions*, Proceedings of 8th International School-Seminar On The Actual Problems Of Microworld Physics, Gomel, 2003, this issue.
- [6] A. Denner, S. Dittmaier, Eur. Phys. J. C9 (1999) 425, hep-ph/9812411.
- [7] M. Moretti, Nucl. Phys. B484 (1997) 3, hep-ph/9604303;
M. Moretti, hep-ph/9606225.
- [8] C. Carimalo, W. da Silva, F. Kapusta, Nucl. Phys. Proc. Suppl. 82 (2000) 391, hep-ph/9909339.
- [9] Shishkina T., Sotsky I., hep-ph/0312208.
- [10] P. De Causmaecker *et al.*, Nucl. Phys. B206 (1982) 53;
F.A. Berends *et al.*, Nucl. Phys. B206 (1982) 61.
- [11] D. Yu. Bardin, N. M. Shumeiko, Nucl. Phys. B127 (1977) 242;
T. V. Kukhto (Shishkina), N. M. Shumeiko, S. I. Timoshin, J. Phys. G: Nucl. Phys. 13 (1987) 725.
- [12] S. Weinzierl, NIKHEF-00-012, hep-ph/0006269.
- [13] L.N.Lipatov and G.V. Frolov ZHETV Pis. Red. 10 (1969) 399., JETP Letters 10 (1969) 254;
V.G. Serbo, ZHETF Pis. Red. 12(1970)33;
H.Cheng and T.T.Wu, Phys. Rev. D1(1970)3414.
- [14] K. Hagiwara *et al.*, Nucl. Phys. B282 (1987) 253.
- [15] G. Belanger *et al.*, Eur. Phys. J. C13 (2000) 283, hep-ph/9908254.
- [16] G. Gounaris *et al.*, "Physics at LEP2" v.1 (1992) 525, hep-ph/9601233.
- [17] A. Denner, S. Dittmaier, M. Roth, D. Wackeroth, Nucl. Phys. B560(1999) 33, hep-ph/9904472.
- [18] A. Denner, S. Dittmaier, M. Roth, D. Wackeroth, Eur. Phys. J. C20(2001) 201, hep-ph/0104057.
- [19] I. Marfin, V. Mossolov, T. Shishkina, hep-ph/0305153.
- [20] I. Marfin, V. Mossolov, T. Shishkina, LC-PHSM-2003-085, hep-ph/0304250.
- [21] I. Marfin, V. Mossolov, T. Shishkina, DESY-PROC-2003-2 384, eConf C030626:FRAP11 (2003) , hep-ph/0308317.

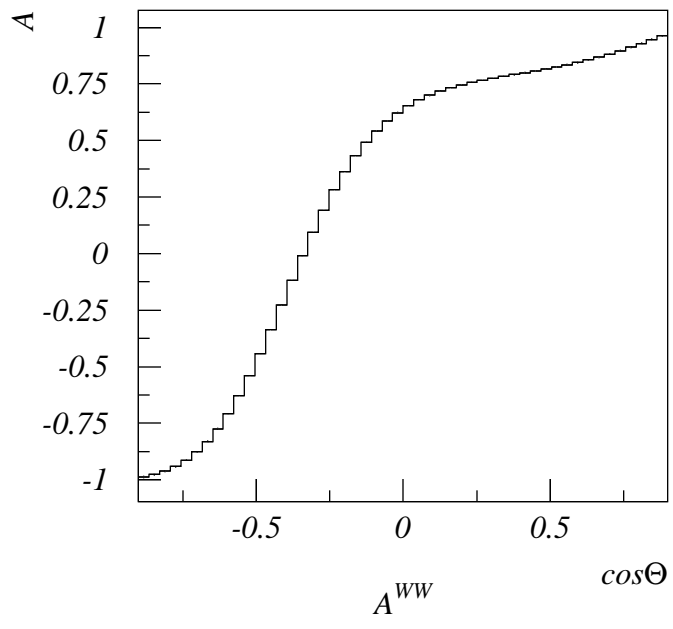
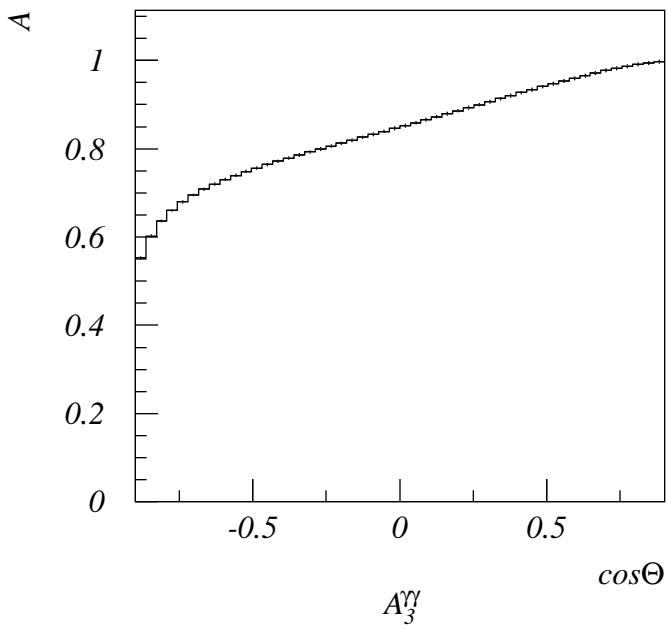
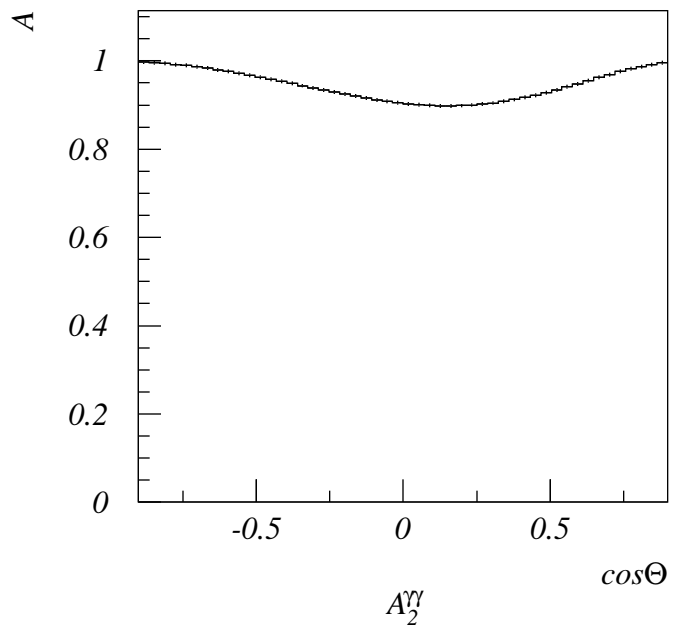
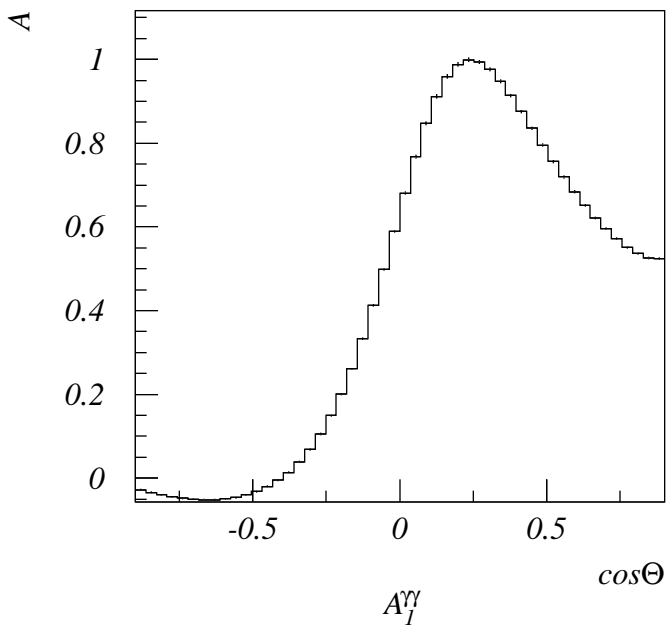


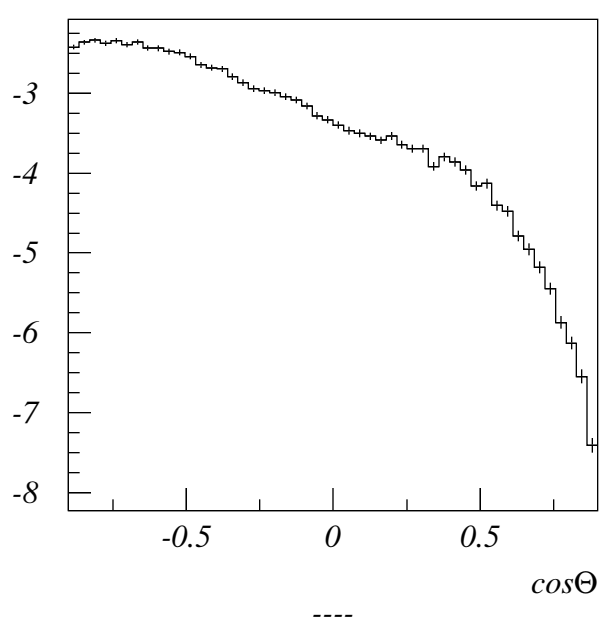
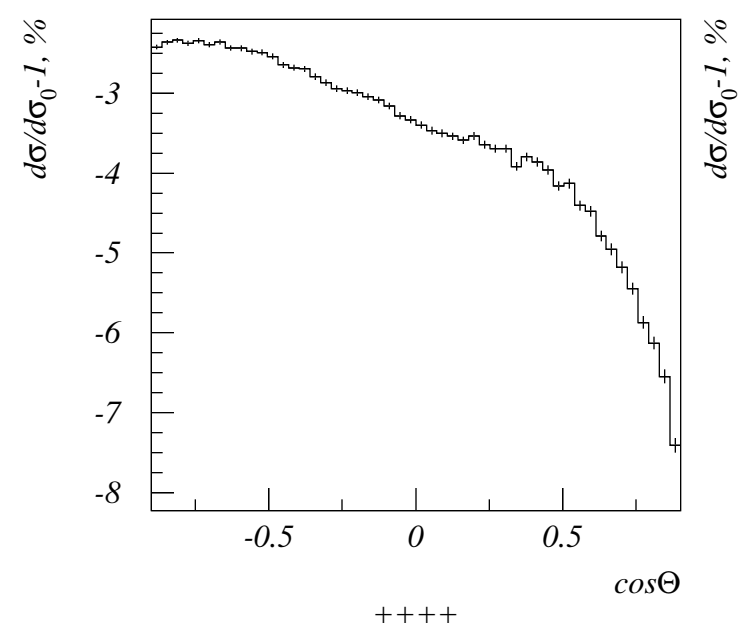
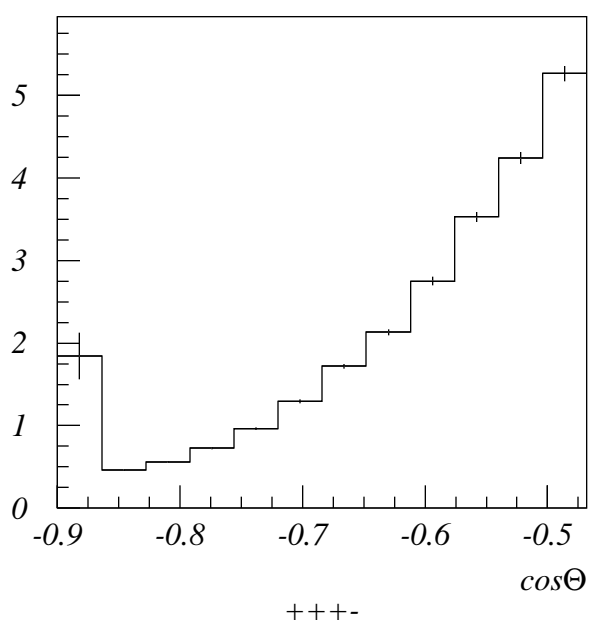
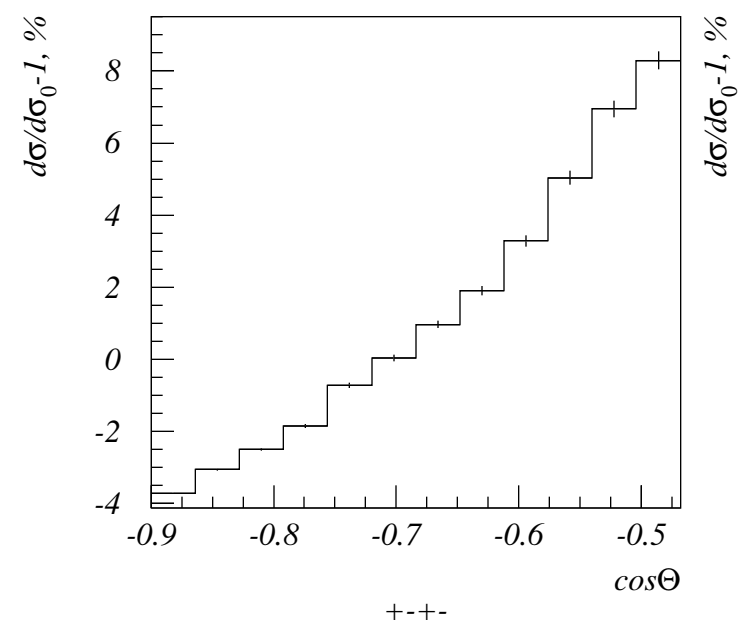


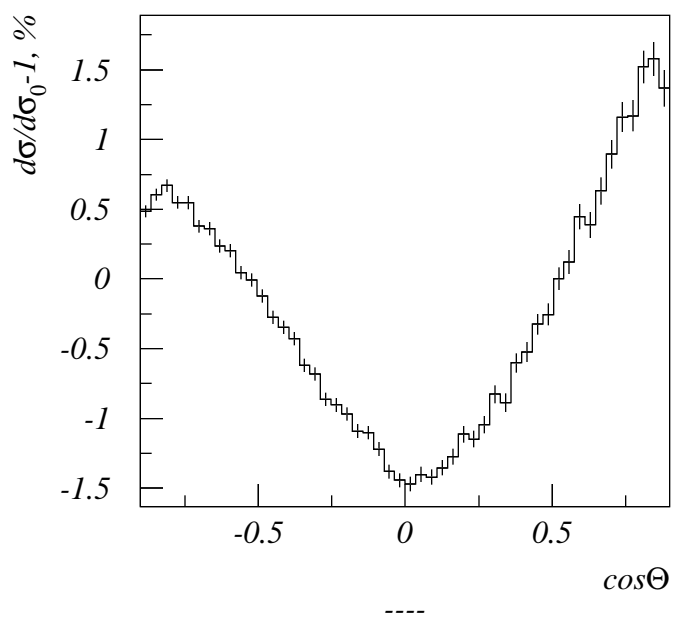
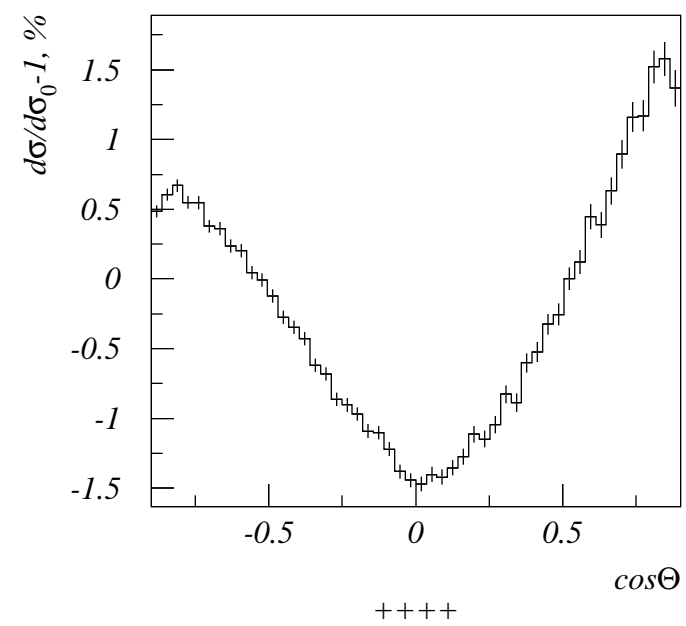
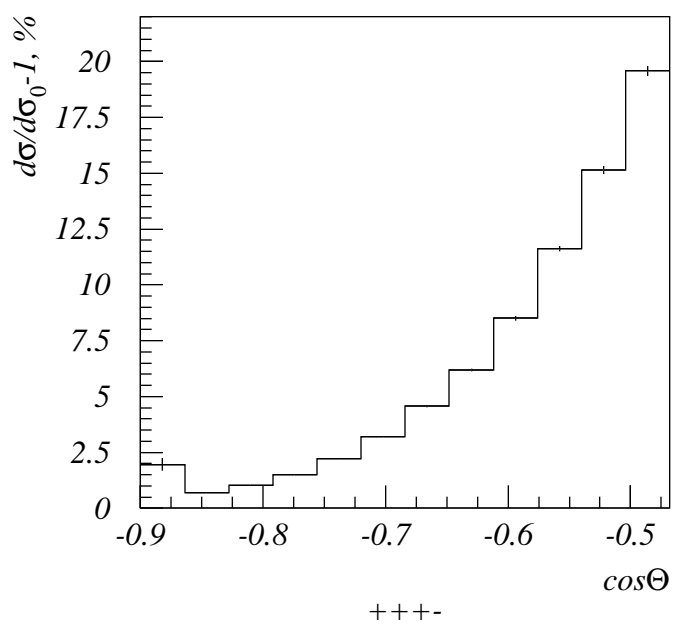
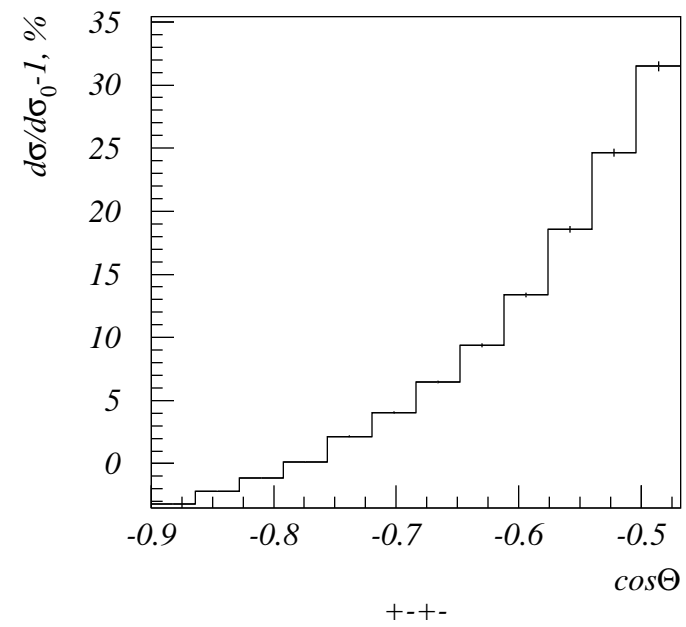


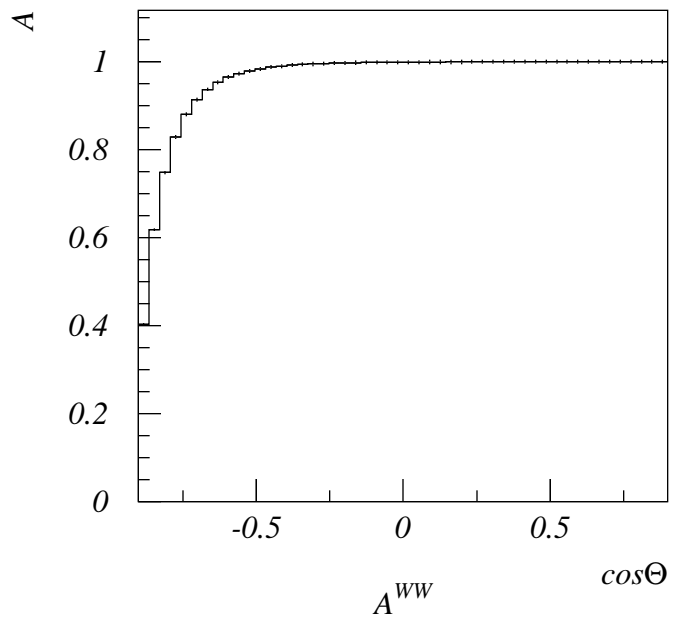
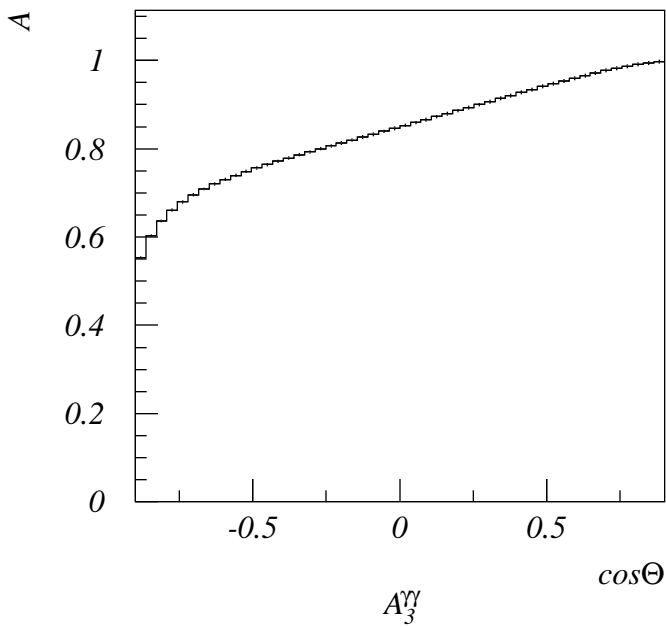
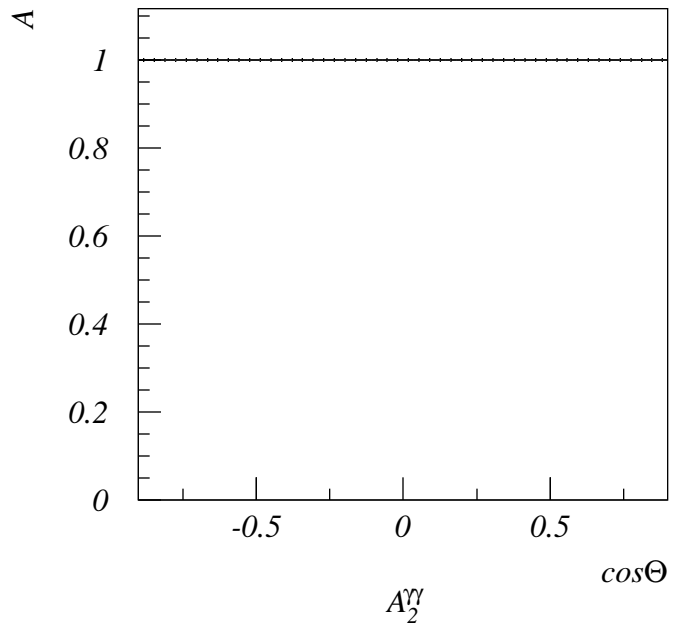
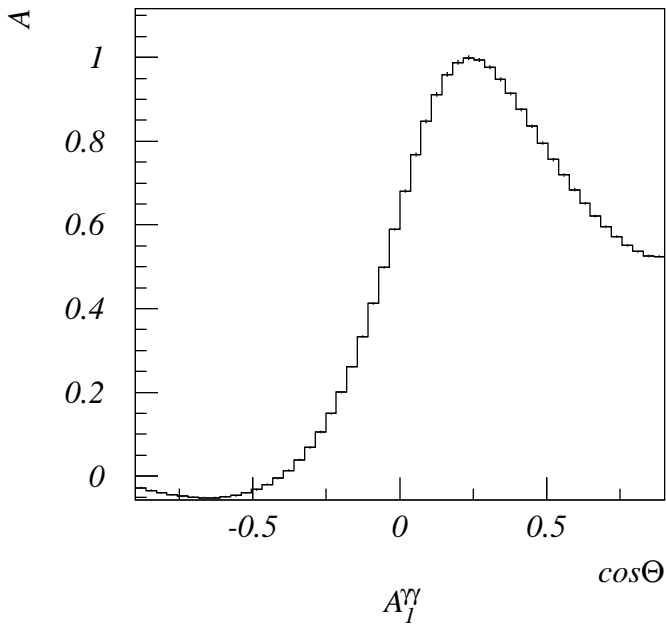


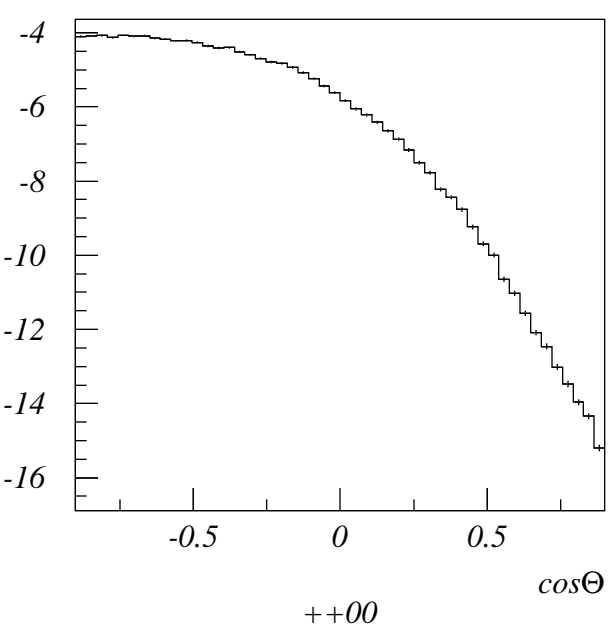
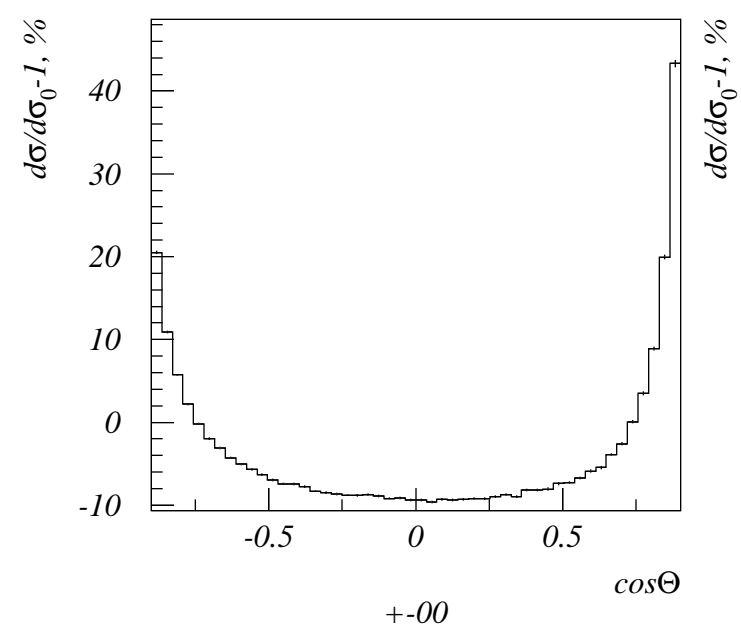
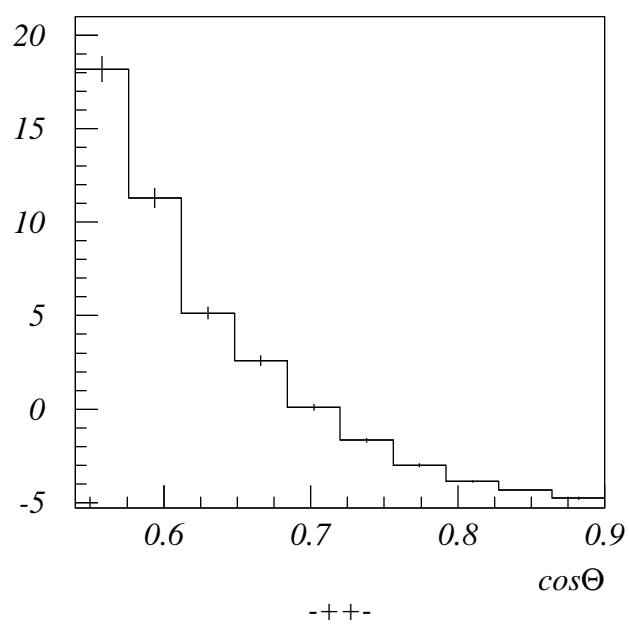
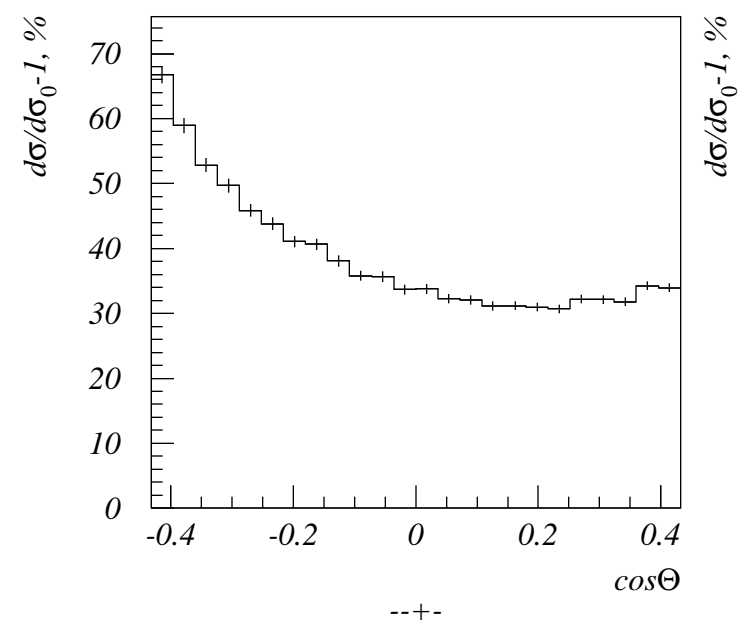


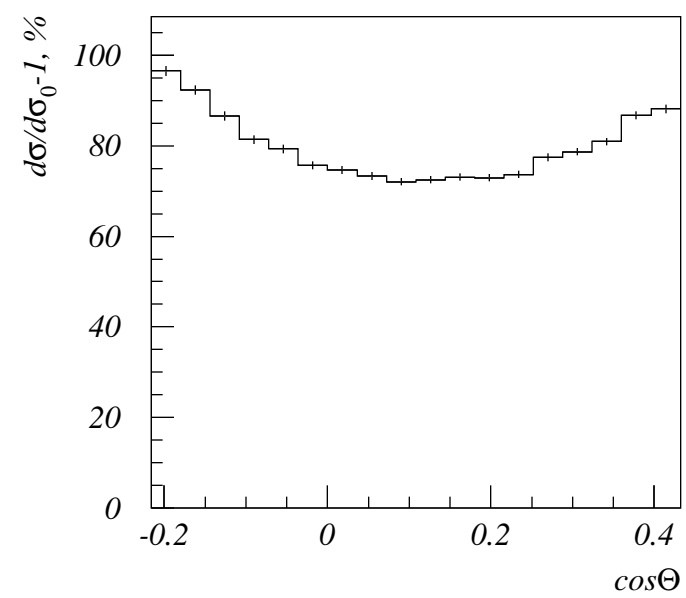




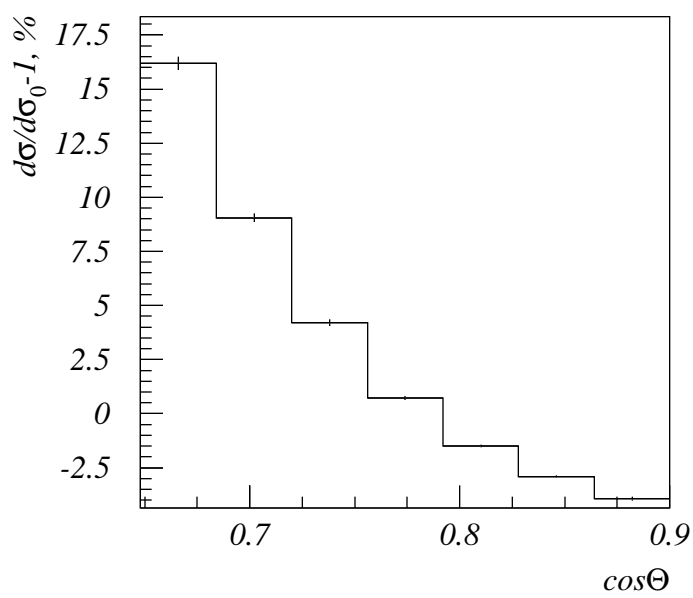




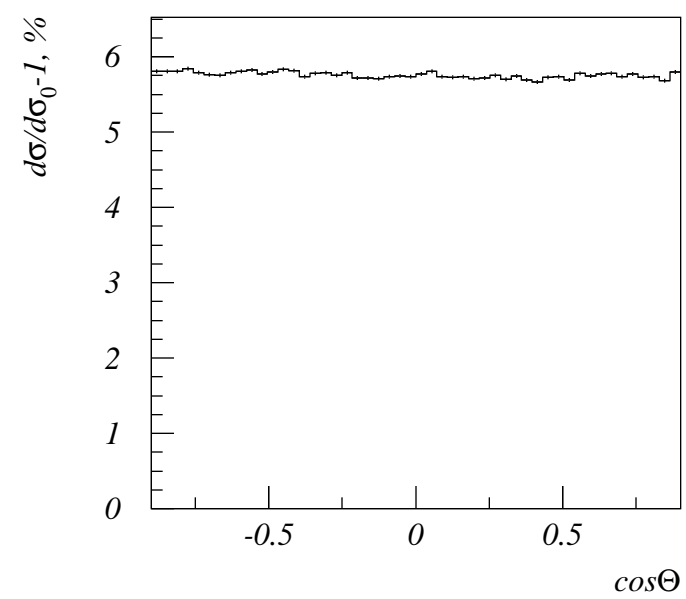




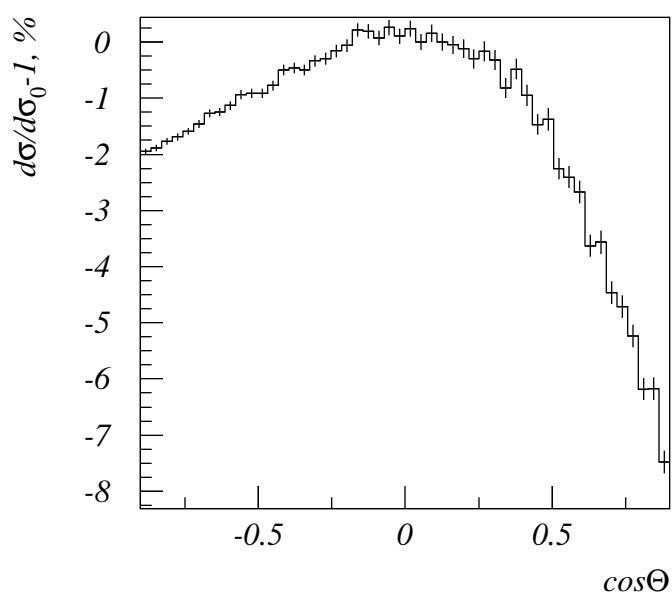
--+-



-++-



+-00



++00

